Linear Control with delay scheduling of a under actuated unstable dynamic system

AUTHOR:
Eng. HELIO SNEYDER ESTEBAN VILLEGAS

DIRECTOR:
professor CARLOS BORRAS PINILLA. PhD., MSc

CO-DIRECTOR:
Professor NEJAT OLGAC. PhD., MSc

CO-DIRECTOR:
Professor DANIEL SIERRA BUENO. PhD., MSc.

Research group in Dynamics, Control and Robotics, DICBOT-UIS

Industrial University of Santander

Bucaramanga, May 2021

Content Table

Tables List

Figure List

Equation List

1. Introduction

The “Delay scheduling” is a modification of linear control laws. This is a recent novel control technique that uses the CTCR paradigm (Cluster treatment of characteristic roots) to increase the robustness of the controllers by the tuning of gain. This gain makes the system more resilient and robust to the presence of a delay; it can reduce overshoots and is very useful when digital system communication protocols are used.

The Pendubot mechanics in the most unstable equilibrium point become extremely nonlinear dynamic. This makes that the application of only linear controllers become a challenge, it has to be solved in the development of the project including the presence of a transport delay.

The transport delay is very common in almost all digital systems. This difference of time between the real signal and the signal can be observed or generated. Transport delays make more unstable a controller and can limit the use of a feedback loop controller in many real industrial applications.

This thesis project brings an opportunity to contribute to the state of art in this hot research area, produce libraries of “Delay scheduling”, and insight on the stability of time-delayed dynamic systems and create an experimental prototype to apply other control laws.

This is the motivation of the research group DICBOT to develop and generate real products with high impact, creating a prototype to help in control teaching as well as research on the stability of nonlinear dynamic with time-delayed systems among others, applied to real dynamic problems as well as provided a solution to industries applications.

Therefore, this research project is a study, development, and application of the “Delay scheduling” approach in an inverted articulated pendulum (Pendubot) experimental

testbed, controlled with PID, PQG, and H∞ control techniques. The “Delay scheduling” control approach will be validated applying the three control techniques in a real prototype experiment and later induce a time delay to prove the effectiveness of the “Delay scheduling” on a design of the two links under an actuated plant.

Remarks: This is the first time, it has been proposed that use the CTCR paradigm implemented and validating on the Pendubot, as far we know.

1. Description of the project

1.1 Tittle

Linear Control with delay scheduling of an under actuated dynamic system

1.2 Project's Director

- Professor: Carlos Borras Pinilla. Ph.D.., MSc.
- Professor: Universidad Industrial de Santander. UIS- Colombia
- School of Mechanical Engineering.

1.3 Project's Co-director

- Professor: Nejat Olgac. Ph.D., MSc.
- Professor of University of Connecticut- USA
- Department of Mechanical Engineering

1.4 Project's Co-director

- Professor: Daniel Alfonso Sierra Bueno. Ph.D.
- Professor: Universidad Industrial de Santander. UIS- Colombia.
- School of Electrical, Electronic and Telecommunications Engineering

1.5 Interested entities in the project

- UIS (Industrial University of Santander)
- UCONN (University of Connecticut)

1.6 Cost of the project

The project has a total cost of $ 41.155.765.oo (11.000. USD) (See details in cost section)

2. Problem Statement

Most of the electronics, control and automation of industrial systems have a transport delay. This delay is a lag between the observed signal and the original signal (Olgac & Sipahi, 1995). This can be caused by the sensor and actuators. Either in some industrial dynamic actuators or some engineering problems, the delay can reach a value of ten seconds.

The problems caused by a high delay are the following:

- Reduce the range of possible gains in a controller
- Increase the overshoot of controllers
- In some cases make a system unstable using classical controllers.

In consequence of these effects caused by delays, in these years the delay become hot research and recurrent investigation topic as can be seen in the following figure.

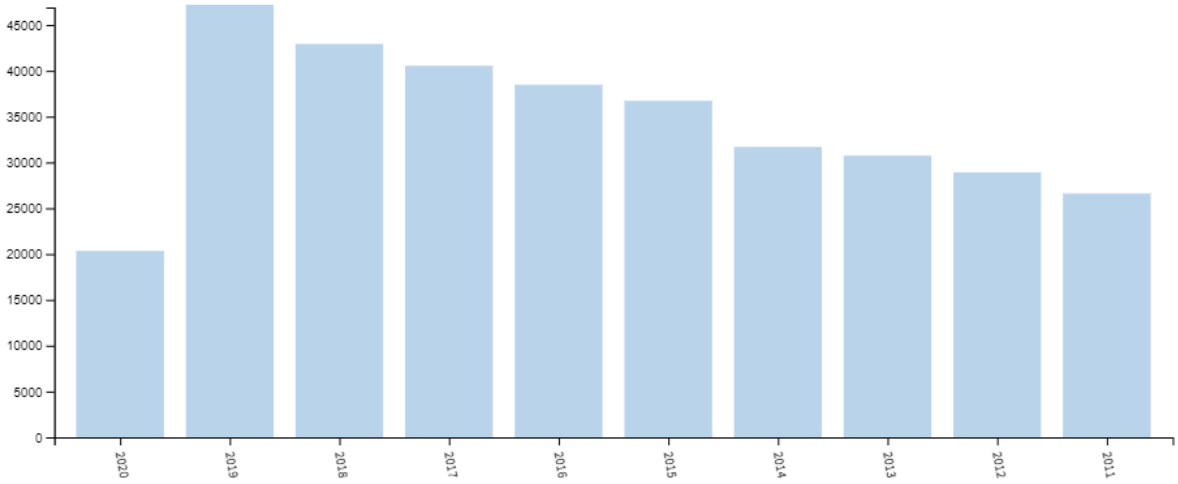

Figure 1. The number of scientific publications per year in the delay topic (Web of Science, n.d.)

This causes that at this moment the investigation of delays is still in progress and there are some applications and improvements in many fields that have not been considered.

3. Justification

3.1 Research Question

Can the “Delay Scheduling” method increase the robustness of classical controllers to handle a significant delay value in the Pendubot prototype?

3.2 Detailed Justification

To solve the problem of the delay one of the most common solutions is to design a robust control that neglects the effect of the delay and other disturbances. This solution has some problems, one of these is that an advanced control technique requires a high computation capacity and reduces the setting times.

Another alternative is to use “Delay scheduling” this technique uses the CTCR paradigm to determine the stability pockets of a feedback-controlled system. These pockets determine the delay range that the system can handle. The idea of this control Technique is to increase the size of the stability pockets and at the same time improve the behavior of the controller (Albertos & Garcia, 2007).

The principal advantage of this technique is that Colombia is still in an automation process for their industries. This produces that the most used controller only can execute PID controllers and their variations. Considering this the use of a technique that allows increasing the robustness of the controllers most used in the country.

The selection of the other two control techniques (LQG and H∞) was defined because don’t require states feedback, are linear, and can be written in the S domain. This selection is suitable to apply the delay scheduling and the implementation of the controllers.

The Pendubot was selected because it is an extremely nonlinear system. This fact and the under-actuated condition of the Pendubot makes that controlling this prototype with linear

controllers became a challenging work. Another characteristic of interest in the Pendubot is that can change the operation zone, passing from unstable to an extremely stable system. This can help in future projects developed by the University.

4. Objectives

4.1 General Objective

Assess the behavior of the control laws PID, LQG, and H∞ with "Delay scheduling" in an under-actuated and unstable pendulum platform using Simulink and Arduino.

4.2 Specific Objective

- Build a nonlinear mathematical model of the unstable under-actuated pendulum based on the real prototype and using physical variables obtained with a grey box identification method.
- Apply the control laws in the prototype without any delay, tuning the controllers in continuous space and using a linearized model of the Pendubot
- Apply the delay scheduling in all the previously designed controllers, inducing a delay based on the results of the CTCR method, comparing the results with the previously tuned controllers.

5. State of art

5.1 Linear control techniques on inverted pendulums

The pendulum-based systems are a common topic in control research. Due to this, many pendulum-based systems were controlled using linear techniques. The most basic technique used to control inverted pendulums is the PID controller and its variations.

5.2 PID Controllers on inverted pendulums

The PID controller in inverted pendulums can be applied in continuous or discrete form and is modified to increase the robustness. The most basic form of PID appears in figure 2 (Olgac & Sipahi, 1995).

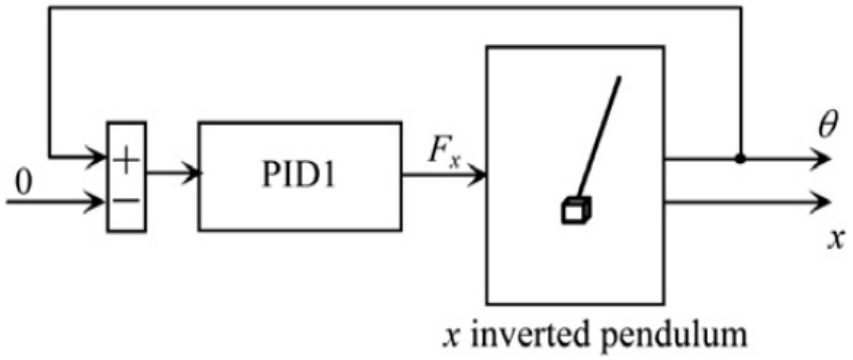

Figure 2. PID Basic structure on the inverted pendulum (Olgac & Sipahi, 1995)

This setup ensures the equilibrium of the pendulum without any control over the displacement of the car. Applying the following control equation (Spong & Block, 1995):

$$F_x = K_p * e(t) + K_p * \int e(t)\ dt + K_p * \frac{de(t)}{dt}$$

Equation 1. PID Control Law

To improve the performance of this structure several methods that modify the gains of the system are implemented. That is the case of the PSO (particle swarm optimization) algorithms which are used as an optimization algorithm that changes the gains of the controller over time (Spong & Block, 1995).

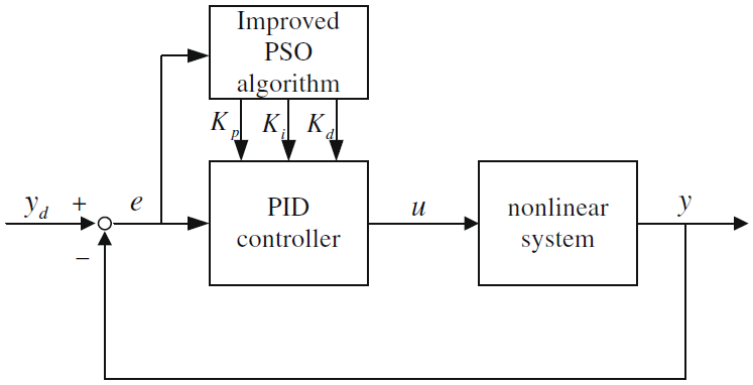

Figure 3. PID Basic structure improved with PSO algorithm (Olgac & Sipahi, 1995)

The previous structures ensure the equilibrium of the system without controlling the car displacement. Therefore, structures that apply multiple loops were created as it appears in figure 4 (Spong & Block, 1995).

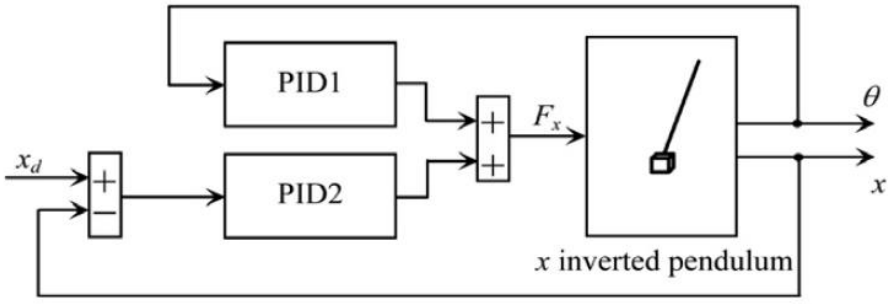

Figure 4. PID structure improved with a second loop to control car displacement (Spong & Block, 1995)

The PID control in figure 4 uses the second loop as decoupled systems which means faster responses but increases the overshoot (Spong & Block, 1995).

Another option is the cascade structure. This case also uses two controllers with the difference that the internal loop ensures the displacement of the base and the second

controls the equilibrium at the same time that interacts with the internal PID. The advantages of the cascade controller are lower overshoots and reduced instability caused by the aggressive change of the set point.

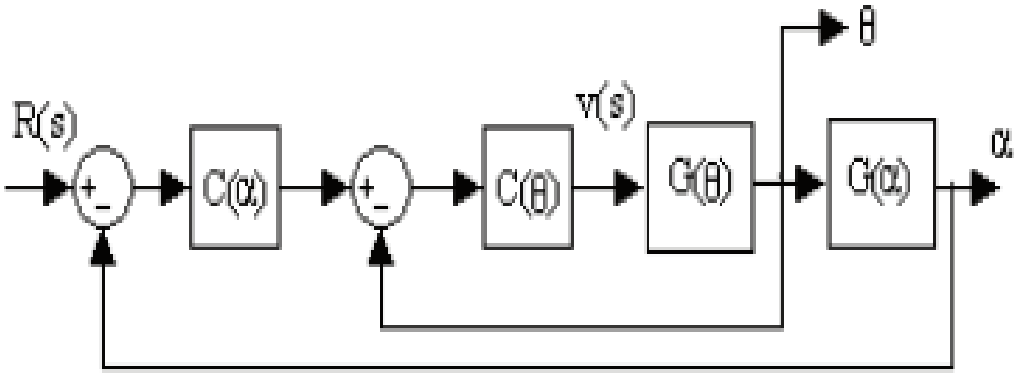

Figure 5. PID cascade structure for inverted pendulum (Spong & Block, 1995))

The PID controller can be modified in several ways to produce new structures and additionally, can be mixed with other controllers. This is the case of the PID mixed with the LQR controller. This controller can control the car position with a faster response than the previous controllers and at the same time ensure the stability of the pendulum with better performance due to the LQR loop (Zhang, M., & Tarn, T. J. (2002)).

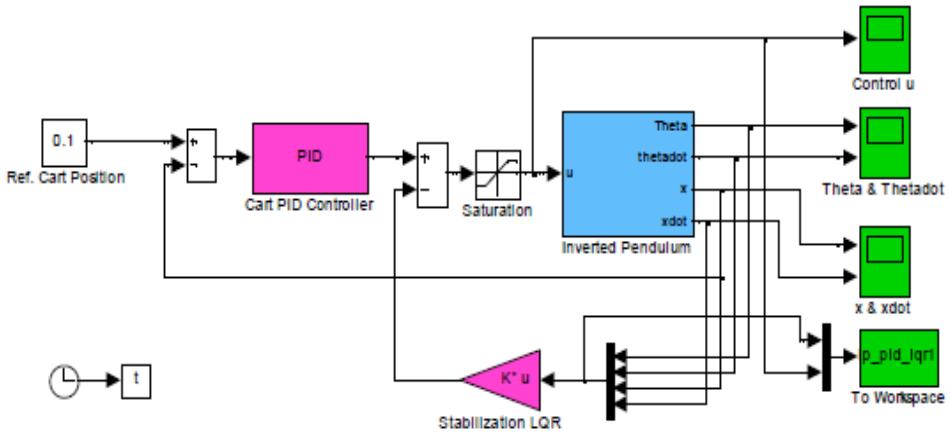

Figure 6. PID mixed with LQR in a two-loop structure (Brian, A., & Jhon, M. (1990))

5.3 LQR Controllers on inverted pendulums

The LQR is a powerful controller highly used on systems with stringent requirements. This technique uses the mathematical model of the system and the Q and R matrices to find the optimal gains. This control technique is applied as a regulator or as a servo controller. When the LQR is used as a regulator, the applied structure can be observed in figure 7.

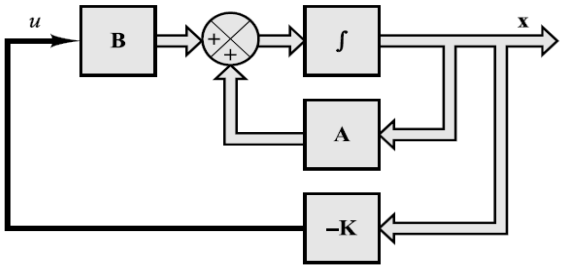

Figure 7. LQR controller as regulator (Ogata, K. (2010))

As a regulator, the LQR controller is calculated using a Q square matrix with the size equal to the number of states and an R square matrix with the size equal to the number of control inputs. The regulator structure is used to hold the system on an equilibrium point and reject the perturbations.

When path tracking is required, the servo controller structure is used. This structure requires the implementation of an extra state that is the integration of error. This

modification ensures a zero steady-state error. For the case of an inverted pendulum, the extra state refers to the car position. The diagram of this structure is shown in figure 8.

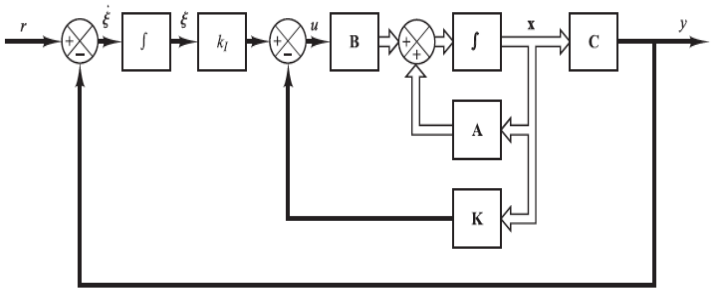

Figure 8. LQG Controllers on inverted pendulums

The LQG controller is the combination of an LQR controller and a Kalman filter. This technique is highly used on inverted pendulums since it can be applied without measuring all the states.

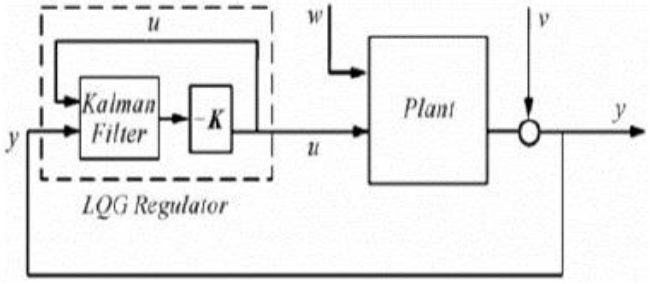

Figure 9. Block Diagram of LQG Controller (Banerjee & Pal, 2018)

The main advantage of Kalman filters in linear dynamic systems is that they can be used to estimate the states of the system from input and output information of the model. Additionally, it is possible to add noise to the ideal system. One common way to implement the LQG controller in inverted pendulums is shown in the following figure:

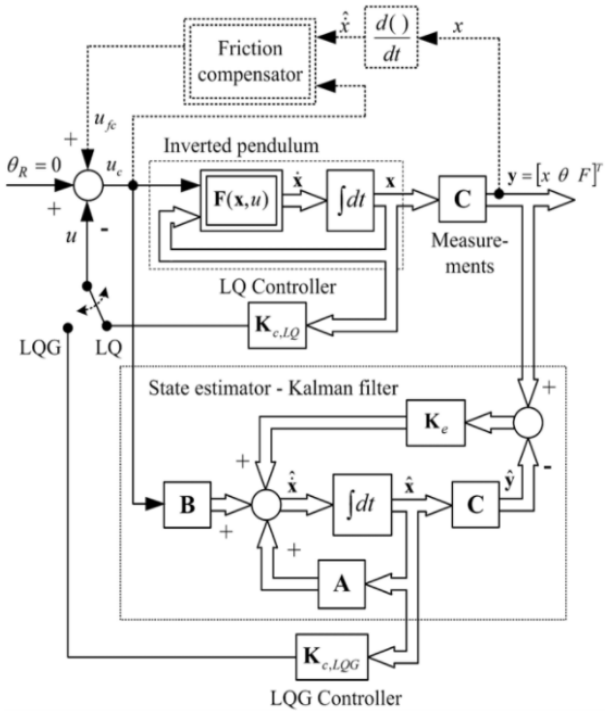

Figure 10. Block Diagram of LQG Controller implemented in an inverted pendulum (Žilić et al., 2009)

Where it includes the LQG controller and a compensator for friction effects. In this case, it is assumed that all state variables are available for feedback. The state feedback controller for the linear time-invariant single-input-multiple-output system is designed such that it brings the state trajectory x to the equilibrium point. For this case, the authors conclude that the LQG controller can effectively suppress the external disturbance and keep the pendulum deflection angle close to zero, even without the friction compensator.

5.4 Pendubot

The Pendubot is an underactuated mechanical system that is commonly used for nonlinear control education to bring the non-actuated link into the vertical unstable equilibrium. It is defined as a planar two-link manipulator robot with the actuated first link and its dynamics can be described using Lagrangian mechanics. The main goal is to design a feedback control law that ensures stable oscillations of the second link, which is the exponential

orbital stability of a periodic motion. To achieve this, it is important to remark that it should be possible to achieve any desired motion.

5.4.1 Pendubot Control

To control this complex system, several methods have been implemented. Those include methods that use energy-based controllers, hybrid controllers, and reduced-order stable controllers.

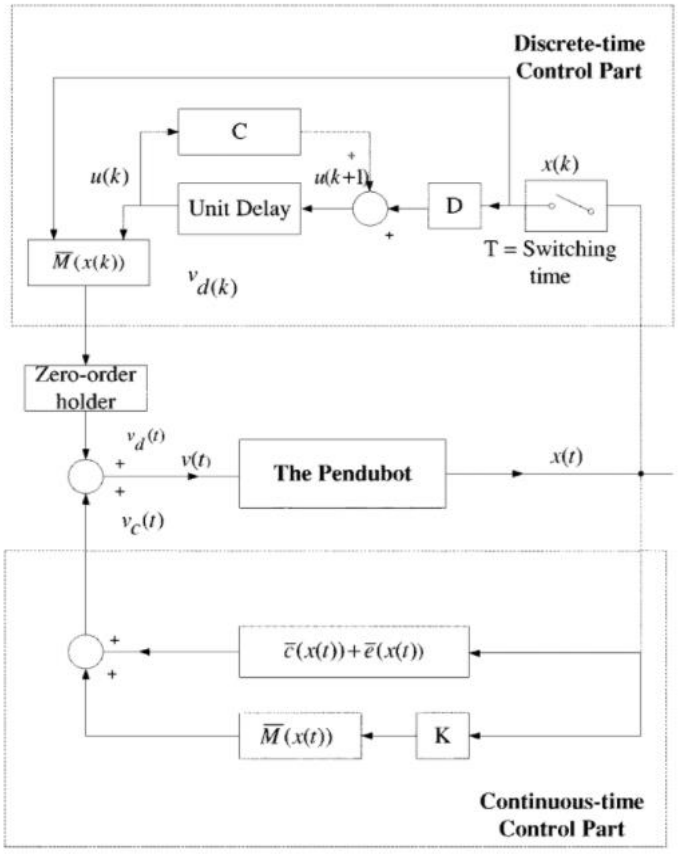

Figure 11. Block Diagram of pendubot with a hybrid controller (Zhang & Tarn, 2002)

The main conclusion of these attempts is that the Pendubot is a simple underactuated mechanical system that shows second-order nonholonomic properties, which makes it a

complex system to control, being that the reason why further methods might be implemented to keep improving the approaches and results.

5.5 Time Delay

Time-delay systems, TDS, are also known as after effect or dead-time systems, hereditary systems, and equations with deviating argument or differential-difference equations. These kinds of systems are part of the class of functional differential equations FDEs that are infinite-dimensional. It helps to increase expectations of dynamic performances since these models behave more similar to a real process. Moreover, the delay properties studies show benefits for control with the voluntary introduction of delays.

6. Theoretical framework

6.1 Transfer Function (Ogata, 2010)

In a linear system represented by a differential equation, the time-invariant transfer function is the ratio of the Laplace transform of the output or response function, assuming that the all-initial conditions are zero.

$$a_0 y^{(n)} + a_1 y^{(n-1)} + \cdots + a_{n-1}\dot{y} + a_n y = b_0 y^{(m)} + b_1 y^{(m-1)} + \cdots + b_{m-1}\dot{x} + b_m y \quad (n \geq m)$$

Equation 2. Differential equation of a linear time-invariant system

Where the input and the output of the system are x, y respectively.

$$Transfer\ function = G(s) = \frac{\mathcal{L}[output]}{\mathcal{L}[input]}\Big|_{zero\ initial\ conditions}$$

$$= \frac{Y(s)}{X(s)} = \frac{b_0 s^m + b_1 s^{m-1} + \cdots + b_{m-1}s + b_m}{a_0 s^n + a_1 s^{n-1} + \cdots + a_{n-1}s + a_n}$$

Equation 3. The transfer function of the nth-order system

If the denominator the power of s of the transfer function is n, then is called an nth-order system.

6.2 State Space (Ogata, 2010)

State-space is a mathematical model of a physic system, which represented throw differential equation of the relation between input, output, and state variables. The elements of the dynamic system must memorize the values of the input for $t \geq t_1$.

In a multiple-input, multiple-output system, better known as a MIMO system that has ***n*** integrator, and ***r*** inputs $u_1(t), u_2(t), \ldots, u_r(t)$, the ***m*** outputs $y_1(t), uy_2(t), \ldots, y_m(t)$. The

state variables of the n outputs of the integrators are $x_1(t), x_2(t), \dots, x_n(t)$, and the system can be defined by

$$\begin{aligned}\dot{x}_1(t) &= f_1(x_1, x_2, \dots, x_n; u_1, u_2, \dots, u_r; t)\\ \dot{x}_2(t) &= f_2(x_1, x_2, \dots, x_n; u_1, u_2, \dots, u_r; t)\\ &\vdots\\ \dot{x}_n(t) &= f_n(x_1, x_2, \dots, x_n; u_1, u_2, \dots, u_r; t)\end{aligned}$$

Equation 4. State space

$$\begin{aligned}y_1(t) &= g_1(x_1, x_2, \dots, x_n; u_1, u_2, \dots, u_r; t)\\ y_2(t) &= g_2(x_1, x_2, \dots, x_n; u_1, u_2, \dots, u_r; t)\\ &\vdots\\ y_m(t) &= g_m(x_1, x_2, \dots, x_n; u_1, u_2, \dots, u_r; t)\end{aligned}$$

Equation 5. Outputs of the system

$$\boldsymbol{x}(t) = \begin{bmatrix} x_1(t) \\ x_2(t) \\ \vdots \\ x_n(t) \end{bmatrix}, \qquad \boldsymbol{f}(\boldsymbol{x}, \boldsymbol{u}, t) = \begin{bmatrix} f_1(x_1, x_2, \dots, x_n; u_1, u_2, \dots, u_r; t) \\ f_2(x_1, x_2, \dots, x_n; u_1, u_2, \dots, u_r; t) \\ \vdots \\ f_n(x_1, x_2, \dots, x_n; u_1, u_2, \dots, u_r; t) \end{bmatrix},$$

$$\boldsymbol{y}(t) = \begin{bmatrix} y_1(t) \\ y_2(t) \\ \vdots \\ y_n(t) \end{bmatrix}, \qquad \boldsymbol{g}(\boldsymbol{x}, \boldsymbol{u}, t) = \begin{bmatrix} g_1(x_1, x_2, \dots, x_n; u_1, u_2, \dots, u_r; t) \\ g_2(x_1, x_2, \dots, x_n; u_1, u_2, \dots, u_r; t) \\ \vdots \\ g_n(x_1, x_2, \dots, x_n; u_1, u_2, \dots, u_r; t) \end{bmatrix}, \quad \boldsymbol{u}(t) = \begin{bmatrix} u_1(t) \\ u_2(t) \\ \vdots \\ u_r(t) \end{bmatrix}$$

Equation 6. System equation

By linearizing the equation around the operating state, the linearized equation of state and the output equation are obtained, as

$$\dot{\boldsymbol{x}}(t) = \boldsymbol{A}(t)\boldsymbol{x}(t) + \boldsymbol{B}(t)\boldsymbol{u}(t)$$

Equation 7. Linearized equation of state

$$\boldsymbol{y}(t) = \boldsymbol{C}(t)\boldsymbol{x}(t) + \boldsymbol{D}(t)\boldsymbol{u}(t)$$

Equation 8. Linearized equation of the output

Where:

- A(t) the state matrix
- B(t) input matrix
- C(t) output matrix
- D(t) direct transmission matrix

This linear continuous-time control system characterized in state space can be represented in a block diagram like in the next figure

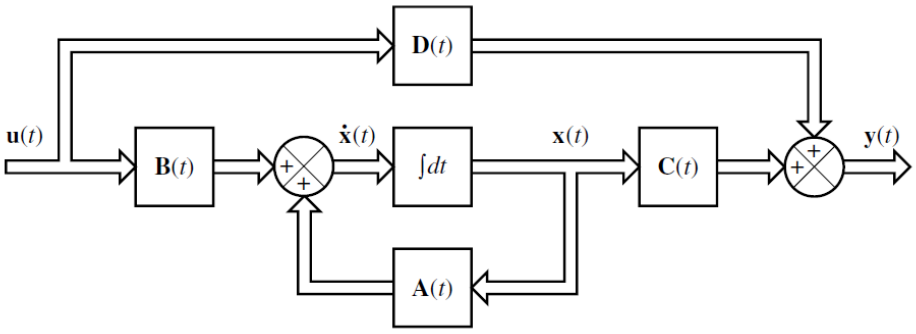

Figure 12. Block diagram of the linear, continuous-time control system represented in state space.

If the system is invariant in the time equation can be simplified as:

$$\dot{\boldsymbol{x}}(t) = \boldsymbol{A}\boldsymbol{x}(t) + \boldsymbol{B}\boldsymbol{u}(t)$$

Equation 9. Linearized equation of state of a time-invariant system

$$\boldsymbol{y}(t) = \boldsymbol{C}\boldsymbol{x}(t) + \boldsymbol{D}\boldsymbol{u}(t)$$

Equation 10. Linearized equation of the output of a time-invariant system

6.3 Lagrange (Murray et al., 1994)

It is a method that allows finding the maximum and minimum of a function of multiple variables with restriction, with which this method can reduce a restricted problem of $\boldsymbol{n}$ variables to one of $\boldsymbol{n} + \boldsymbol{\lambda}$ unrestricted variables, where $\boldsymbol{\lambda}$ are called Lagrange multipliers.

The system can be written as

$$F = \begin{bmatrix} m_1 I & & 0 \\ & \ddots & \\ 0 & & m_n I \end{bmatrix} \begin{bmatrix} \ddot{r}_1 \\ \vdots \\ \ddot{r}_n \end{bmatrix} + \sum_{j=1}^{k} \Gamma_j \lambda_j$$

Equation 11. System dynamics as a vector

Where

- $\Gamma_1, \ldots, \Gamma_k \in \mathbb{R}^3$ They are the basis of the constraint forces and are not necessarily must to be orthonormal.
- $\lambda_1, \ldots, \lambda_k \in \mathbb{R}^k$ The Lagrange multipliers are a factor that gives the relative magnitude of the constrained forces relative to Γ_j.

In a mechanical system, the equation of motion in generalized coordinates $q \in \mathbb{R}^m$ and a Lagrangian L, and the external force Υ_i acting on the ith coordinate can write as show

$$\frac{d}{dt}\frac{\partial L}{\partial \dot{q}_i} - \frac{\partial L}{\partial q_i} = \Upsilon_i \quad i = 1, \dots, m$$

Equation 12. Lagrange's equation

Without constraints can choose q to a be a component of *r*, by

$$T = \frac{1}{2}\sum m_i \left\| \dot{r}_i^2 \right\|$$

Equation 13. Find q in r components

That able to rearrange the Lagrange equation as

$$\frac{d}{dt}\frac{\partial L}{\partial \dot{q}} = \frac{\partial L}{\partial q} + \Upsilon$$

Equation 14. Lagrange's equation in vector form

6.4 PID Control (Ogata, 2010)

When the mathematical model of the plant is derivable, can determine, the parameters of the controller that can the transient and steady-state specifications of the closed-loop system.

The PID controller parameter can be tuned based on the Ziegler and Nichols rules, to determine the values of the proportional gain K_p, integral time T_i, and derivative time T_d based on the transient response characteristics of a given plant, these values can be found with the next equations

Type of Controller	K_p	T_i	T_d
P	$\frac{T}{L}$	∞	0

PI	$0.9\frac{T}{L}$	$\frac{L}{0.3}$	0
PID	$1.2\frac{T}{L}$	2L	0.5L

Table 1. Ziegler–Nichols tuning rule based on step response of plant

The function C(s)/U(s) can approximate to first-order system with a transport lag as follows:

$$\frac{C(s)}{U(s)} = \frac{Ke^{-Ls}}{Ts+1}$$

Equation 15. First-order system with transport lag

Of the equation table, obtain

$$G_c(s) = K_p\left(1 + \frac{1}{T_i s} + T_d s\right) = 1.2\frac{T}{L}\left(1 + \frac{1}{2Ls} + 0.5Ls\right) = 0.6T\frac{\left(s+\frac{1}{L}\right)^2}{s}$$

Equation 16. Plant with PID controller

This PID controller has a pole at the origin and double zeros at $s = -1/L$.

6.5 Quadratic Optimal Regulator Systems - LQR Control (Ogata, 2010)

This method gives a systematic way to find the state feedback control gain matrix; this is a plus over the pole-placement method.

Given the equation

$$\dot{\boldsymbol{x}} = \boldsymbol{Ax} + \boldsymbol{Bu}$$

Equation 17. State-space system

$$\boldsymbol{u}(t) = -\boldsymbol{K}\boldsymbol{x}(t)$$

Equation 18. The K matrix of the control vector

$$J = \int_0^\infty (\boldsymbol{x}^*\boldsymbol{Q}\boldsymbol{x} + \boldsymbol{u}^*\boldsymbol{R}\boldsymbol{u})dt$$

Equation 19. The performance index equation

Where,

- **Q** is a matrix that could be a real symmetric, or a Hermitian (positive-definite or positive-semidefinite)
- **R** is a matrix that could be a real symmetric or a positive-definite Hermitian
- **u**(t) in this case is unconstrained

Is important that have in mind that the Q and R matrix determine the cost of energy and the relative significance of the error.

The optimal configuration is shown in the next block diagram

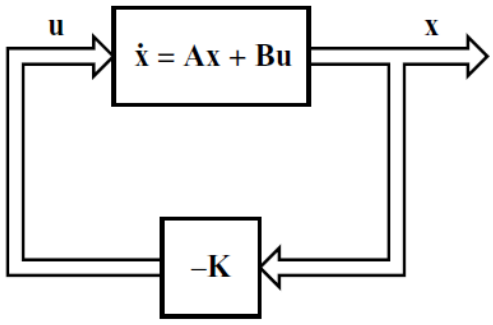

Figure 13. Quadratic optimal regulator configuration

Substituting equation 14 into equation 13 yields

$$\dot{\boldsymbol{x}} = \boldsymbol{Ax} - \boldsymbol{BKx} = (\boldsymbol{A} - \boldsymbol{BK})\boldsymbol{x}$$

Equation 20. System equation with K matrix

Assume that the ***A - BK*** matrix is stable and for hence its eigenvalues have a negative real part.

Substituting Equation 14 into 15 gives

$$J = \int_0^\infty (\boldsymbol{x}^*\boldsymbol{Qx} + \boldsymbol{x}^*\boldsymbol{K}^*\boldsymbol{RKx})dt = \int_0^\infty \boldsymbol{x}^*(\boldsymbol{Q} + \boldsymbol{K}^*\boldsymbol{RK})\boldsymbol{x}\, dt$$

Equation 21. The performance index equation in terms of K

To solve this integration and if that matrix ***A - BK*** is stable, there must be at least one positive definite matrix P that satisfies the following equation, for the system to be stable

$$(\boldsymbol{A} - \boldsymbol{BK})^*\boldsymbol{P} + \boldsymbol{P}(\boldsymbol{A} - \boldsymbol{BK}) = -(\boldsymbol{Q} + \boldsymbol{K}^*\boldsymbol{RK})$$

Equation 22. System equation with K and P matrix

The new J is rewritten as

$$J = \int_0^\infty \boldsymbol{x}^*(\boldsymbol{Q} + \boldsymbol{K}^*\boldsymbol{RK})\boldsymbol{x}\, dt = -\boldsymbol{x}^*\boldsymbol{Px}|_0^\infty = -\boldsymbol{x}^*(\infty)\boldsymbol{Px}(\infty) + \boldsymbol{x}^*(0)\boldsymbol{Px}(0)$$

Equation 23. The performance index equation in terms of P and x

Equation 19 can be reduced since all the eigenvalues of ***A - BK*** have negative real parts, and therefore $\boldsymbol{x}(\infty)\rightarrow 0$

$$J = \boldsymbol{x}^*(0)\boldsymbol{Px}(0)$$

Equation 24. The performance index equation in terms of P and x(0)

Knowing that ***R*** must be a positive-definite Hermitian or real symmetric matrix, can define ***R*** as multiplication of a transpose ***T**** and ***T*** (nonsingular matrix)

$$\boldsymbol{R} = \boldsymbol{T}^{*}\boldsymbol{T}$$

Equation 25. Definition of R matrix

In addition, the K matrix can rewrite as

$$\boldsymbol{K} = \boldsymbol{T}^{-1}(\boldsymbol{T}^{*})^{-1}\boldsymbol{B}^{*}\boldsymbol{P} = \boldsymbol{R}^{-1}\boldsymbol{B}^{*}\boldsymbol{P}$$

Equation 26. Optimal matrix K

If the performance index in equation 15 is linear and is set by

$$\boldsymbol{u}(t) = -\boldsymbol{K}\boldsymbol{x}(t) = -\boldsymbol{R}^{-1}\boldsymbol{B}^{*}\boldsymbol{P}\boldsymbol{x}(t)$$

Equation 27. The control signal in function of R, B, and P matrix

The matrix P in equation 22 must satisfy equation 16 or the next equation

$$\boldsymbol{A}^{*}\boldsymbol{P} + \boldsymbol{P}\boldsymbol{A} - \boldsymbol{P}\boldsymbol{B}\boldsymbol{R}^{-1}\boldsymbol{B}^{*}\boldsymbol{P} + \boldsymbol{Q} = 0$$

Equation 28. Reduced-matrix Riccati equation

Design steps:

1. Solve equation 24 for ***P***, if the result is a positive-definite matrix, the system is stable, or matrix ***A*** - ***BK*** is stable
2. Use the matrix ***P*** to substitute into equation 22, and the result is the optimal matrix ***K***

The performance index is determined by

$$J = \int_{0}^{\infty} (\boldsymbol{y}^{*}\boldsymbol{Q}\boldsymbol{y} + \boldsymbol{u}^{*}\boldsymbol{R}\boldsymbol{u})dt$$

Equation 29. Performance index in terms of u and R

In addition, the output equation can be replaced by

$$\boldsymbol{y = Cx}$$

Equation 30. Output equation

In the index performance, an rewrite as

$$J = \int_0^{\infty} (\boldsymbol{x^* C^* Q C x + u^* R u})dt$$

Equation 31. Performance index in terms of u, R, and C

6.6 Linear Quadratic Gaussian System - LQG Control

The Linear Quadratic Gaussian System (Brian & Jhon, 1990) (Montoro López, 1996) is combination of a Kalman filter, a Linear Quadratic Estimator (LQE) and a Quadratic Optimal Regulator (LQR). This method facilities the analysis of linear systems with perturbation of withe noise and incomplete states.

The linear dynamic system is given by the next equation

$$\dot{x}(t) = A(t)x(t) + B(t)u(t) + v(t)$$

Equation 32. State-space variables

$$y(t) = C(t)x(t) + w(t)$$

Equation 33. Output system

Where

- X is the variable vector of state-space
- u is the vector inputs
- y is the vector with the available outputs for retro alimentation

- v(t) withe additive Gaussian noise of zero means, with covariance $\hat{Q}(t)\delta(t-\tau)$, where $\hat{Q}$ is nonnegative definite symmetric for all t
- w(t) the measurable additive Gaussian noise of zero means, with covariance $\hat{R}(t)\delta(t-\tau)$, where $\hat{R}$ is nonnegative definite symmetric for all t
- The matrix A, B, C, $\hat{Q}$ and $\hat{R}$ are assumed to have continuous elements

Having presented that v and w are independent processes, $u(t)$ can depend only on the lasts measure $y(t')$, $0 \leq t' \leq t$, the performance index function can be written as

$$J = E\left(x^T(T)Fx(T) + \int_0^T x^T(t)Q(t)x(t) + u^T(t)R(t)u(t)\,dt \right);\ F \geq 0, Q(t) \geq 0, R(t) \geq 0$$

Equation 34. Performance index

Where

- E is the expected value
- T is the final hour (Horizon) can be finite or infinite

Assume that the horizon tends to infinite the first term $x^T(T)Fx(T)$ of the performance index make insignificant and the operator E make a mean of the quadratic integral. To obtain the optimum feedback needs v and w, such as

$$E\left\{\begin{bmatrix} w(t) \\ v(t) \end{bmatrix}\right\} = \begin{bmatrix} 0 \\ 0 \end{bmatrix}$$

$$E\left\{\begin{bmatrix} w(t) \\ v(t) \end{bmatrix}\begin{bmatrix} w(\tau)^T & v(\tau)^T \end{bmatrix}\right\} = \begin{bmatrix} R_{ww} & 0 \\ 0 & R_{vv} \end{bmatrix}$$

Equation 35. E expected value E equation

The process and measurement noises are considered uncorrelated, and the autocorrelations are given by Dirac delta functions. The estimator is given by

$$\dot{\xi} = A\xi + Bu + K_e(y - C)$$

Equation 36. Estimator $\dot{\xi}$

In the last equation, K_e is the solution to the next Riccati equation

$$P_J = Ric\left(\begin{bmatrix} A^T & -C^T R_{vv}^{-1} C \\ -\Gamma R_{ww} & -A \end{bmatrix}\right) = AP_J + P_J A^T + \Gamma R_{ww} \Gamma^T - P_J C^T R_{vv}^{-1} C P_J$$

Equation 37. Riccati equation

$$K_e = P_J C^T R_{vv}^{-1}$$

Equation 38. Riccati solution K_e

In similarly the K_c is the solution of the next equation

$$P_H = Ric\left(\begin{bmatrix} A & BW_2^{-1}B^T \\ -W_1 & -A^T \end{bmatrix}\right) = A^T P_H + P_H A + \mathrm{W}_1 - P_H B W_2^{-1} B^T P_H$$

Equation 39. Riccati equation

$$K_c = W_2^{-1} B^T P_H$$

Equation 40. Riccati solution K_c

The optimum feedback is

$$u = -K_c \xi$$

Equation 41. Optimum feedback LQG

The general block diagram of an LQG is shown below

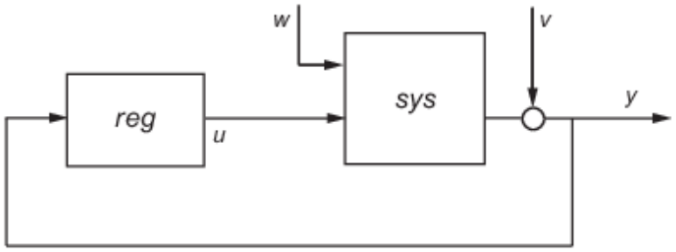

Figure 14. LQG block diagram (MatLab, n.d.)

In addition, can be expressed that an input filter y and an output u, with a Laplace transform,

$$U(s) = F(s)Y(s)$$

Equation 42.Transform to find the control action

$$F(s) = \left[\frac{A - K_e C - BK_c}{-K_c}\right]$$

Equation 43. Laplace transform of a LQG

6.7 The H-Infinity (H∞) Control Technique

The technique name is H-infinity, because the mathematic definition of the problem may be customary in the space H∞, in other words, all functions are bound to the right-half complex plane. This method tries to find how to minimize the H∞-norm of a transfer matrix, which represents the maximum overall frequencies of its largest singular value (Francis, 1987). In a difference with LQR method, the H∞ full state feedback can see how the disturbances affect the plant dynamics (Phillips & Athans, 1994), for this reason, is used to minimize the impact of perturbation in a closed-loop, and this can be measured in terms of stabilization or performance (Sirisha & S. Junghare, 2014).

The rational transfer function matrix G(s) is in H1 if and only if all its poles are in the open left half-plane and it is proper too, in this case, the H1-norm can be defined as (Glover, 2020):

$$\|G(s)\|_\infty = \sup_{Res>0} \sigma_{max}\left(G(s)\right) = \sup_{-\infty<\omega<\infty} \sigma_{max}\left(G(j\omega)\right)$$

Equation 44. H(∞)-norm

Where σ_{max} denotes the largest singular value.

In the case of a single input/single output a system with g(s) as its transfer function, and its H∞-norm, ‖g(s)‖_∞ obtain the maximum value of |g(jω)| and this is the maximum amplification of sinusoidal signals. On another hand, a MIMO system case obtains the system amplification of a vector of sinusoids.

This system with transfer function G(s), has an input vector u(t)∈L_2 (0,∞) and an output vector y (t), with $\bar{u}(s)$ and $\bar{y}(s)$ as Laplace transforms (Glover, 2020).

$$\dot{x}(t) = Ax(t) + Bu(t), \;\; y(t) = Cx(t) + Du(t)$$

Equation 45. State-space

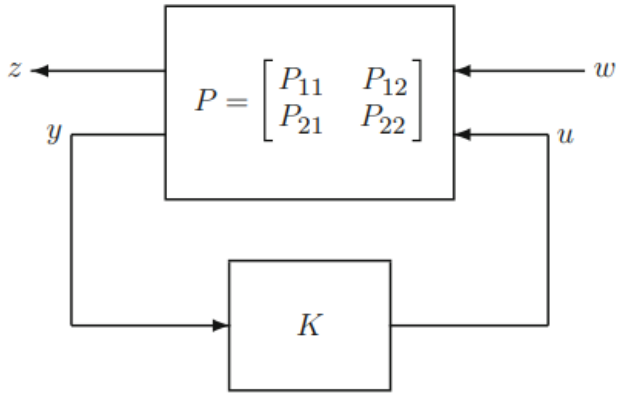

Figure 15. Lower linear fractional transformation: feedback system (Glover, 2020)

With G(s) = D + C (sI - A)$^{-1}$B, denote as (Glover, 2020):

$$G(s) = \begin{bmatrix} A & B \\ C & D \end{bmatrix}$$

Equation 46. G(s) in matrix form

And $\bar{y}(s) = G(s)\bar{u}(s)$ if x (0) =0

In an input signals vector $u(t) \in \mathcal{L}_2(0,\infty)$ or equivalently, $\bar{u}(j\omega) \in \mathcal{L}_2(-\infty,\infty)$, with the corresponding norm $\|u\|_2^2 = \int_0^\infty u(t)^* u(t)dt$ (where x* denotes the conjugate transpose of the vector or a matrix x). For these inputs and outputs, the norm of the system can be expressed as (Glover, 2020):

$$\|y\|_2 \leq \|G(s)\|_\infty \|u\|_2$$

Equation 47. H(∞)-norm of G(s)

A typical control problem is given as (Glover, 2020):

$$\begin{bmatrix}\bar{z}\\ \bar{y}\end{bmatrix} = P\begin{bmatrix}\bar{w}\\ \bar{u}\end{bmatrix} = \begin{bmatrix}P_{11}\bar{w} & P_{12}\bar{u}\\ P_{21}\bar{w} & P_{22}\bar{u}\end{bmatrix}$$
$$\bar{u} = K\bar{y}$$
$$\bar{y} = (I - P_{22}K)^{-1}P_{21}\bar{w}$$
$$\bar{u} = K(I - P_{22}K)^{-1}P_{21}\bar{w}$$
$$\bar{z} = (P_{11} + P_{12}K(I - P_{22}K)^{-1}P_{21})\bar{w}$$
$$=: F_l(P,K)\bar{w} =: T_{z\leftarrow w}\bar{w}$$

Equation 48 Composition of an H infinity delay problem

The lower Linear Fractional Transformation (LFT) is denoted by $F_l(P,K)$

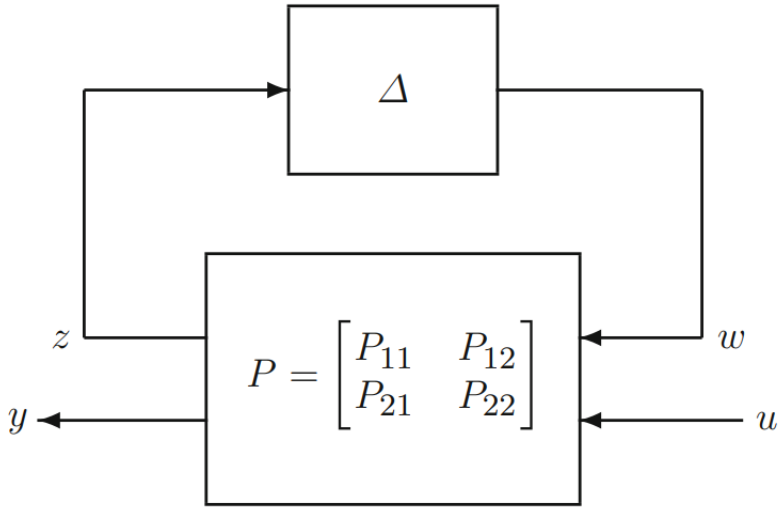

Figure 16. Upper linear fractional transformation (Glover, 2020)

The object of the H∞-control is to catch a transfer function K, which makes it possible to stabilize the closed-loop system and minimizes $\|F_l(P,K)\|_\infty$

6.8 Delay or dead time

The main problem to be solved in this project is the Transport Delay or Dead Time. This characteristic of the dynamic systems transports the variable response at a specific time. This phenomenon cause instability and poor control performance with classical control techniques (Sipahi & Olgac, 2005).

This effect can be seen in fig 17, where the induced delay is of one second on a linear plant.

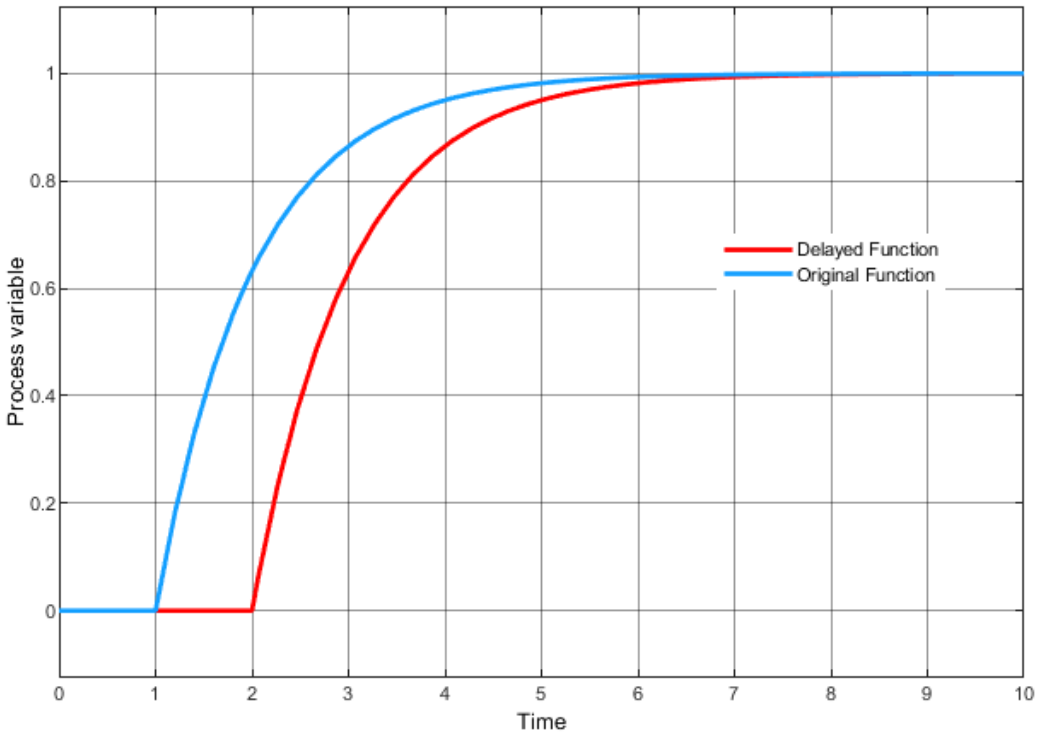

Figure 17. Delay applied on a linear system using MATLAB Simulink

The delays may appear at a different point of the control loop, in fig 18 the three most common delays are shown:

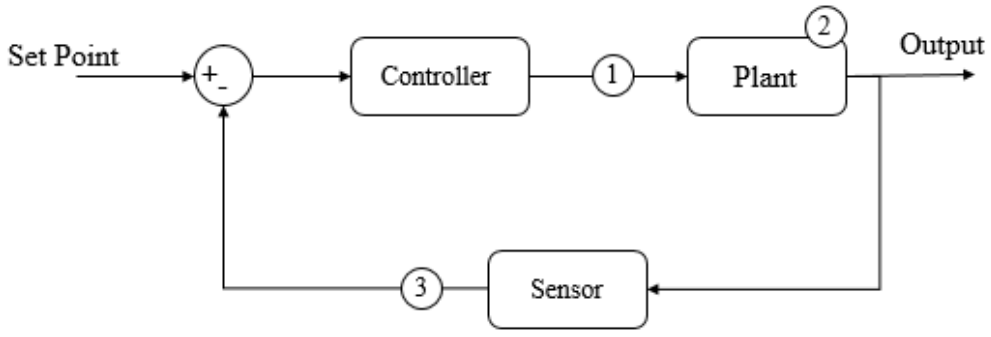

Figure 18. Control Loop with the most common delay cases (Olgac & Sipahi, 1995) (Cavdaroglu & Olgac, 2009)

Case one is the delay between the controller and the plant to be controlled. This delay is caused commonly by the communication of the controller or also the dynamic of the actuators. The second delay is caused by the inner dynamic of the system, this appears when the state equations of the system contain a delay. And the third case appears in the

sensing process of the variables on the clear example for this case is the sensors used in radiotherapy. The three cases increase the limitation in the control design process (Roh & Oh, 1999) (Davison & Tonita, 2005).

The mathematical representation in frequency space of transport delay is the following (Olgac & Sipahi, 1995).

$$D = e^{-\tau s}$$

Equation 49. Transport delay in frequency space

This representation brings accuracy to the model but increases the required resources to carry out some analysis. According to this Rekasius substitution can be used (Albertos & Garcia, 2007)

$$e^{-\tau s} = \frac{1 - Ts}{1 + Ts}$$

Equation 50. Rekasius substitution used by (Albertos & Garcia, 2007)

Both delay representations can be used according to the selected stability analysis.

6.9 Stability analysis methods

To control any delayed dynamic system, it is necessary to determine the stability of the entire system. Hence, many methods to perform an analysis for stability have been developed.

6.9.1 Lyapunov stability

The Lyapunov stability for the delayed system commonly uses the Razumikhin-function approach (Mazenc & Niculescu, 2001). This method is used on systems with the following form:

$$\dot{x}(t) = f\big(x(t)\big) + g(x(t), x(t-\tau), t)$$

Equation 51. System equation

With the system defined the next step is to identify the two conditions used to determine stability. The first condition is that the system, $\dot{x}(t) = f\big(x(t)\big)$ is globally asymptotically stable and a function $V(x)$ and a positive non-decreasing function $\psi(.)$ can be found to satisfy the following asymptotically stable inequality (Mazenc & Niculescu, 2001):

$$\frac{\partial V}{\partial x}(x) f(x) \leq -2\psi(V(x))$$

Equation 52. Globally asymptotically stable system

The next condition requires that a continuous function $\varepsilon(a,b) \in [0,1]$ that satisfy the following inequality (Mazenc & Niculescu, 2001)

$$\left|\frac{\partial V}{\partial x}(a) g(a,b,t)\right| \leq \psi\big(V(x)\big) + \varepsilon(a,b)\psi\big(V(b)\big), \forall (a,b)$$

Equation 53. Second condition for stability

If a feedback system satisfies both conditions will be asymptotically stable and the range of the delay allowed can be determined.

6.9.2 CTCR method

The CTCR paradigm allows determining stability regions in multi-delayed systems according to (Cavdaroglu & Olgac, 2009)(Sipahi & Olgac, 2005)(Zhang & Tarn, 2002). For the Pendubot case, a single delayed system is assumed, so the CTCR paradigm is only used for the one delay case. The CTCR paradigm begins its formulation with a classical time-delayed system with the form (Olgac & Sipahi, 1995):

$$\dot{x} = Ax + Bx(t - \tau)$$

Equation 54. CTCR form, LTI-TDS

$$RT|_{\substack{\omega=\omega_{ck} \\ \tau=\tau_{kl}}} = sgn\left[\left(\frac{ds}{d\tau}\Big|_{\substack{s=\omega_{ck^i} \\ \tau=\tau_{kl}}}\right)\right]$$

$$k = 1, \dots, m \quad l = 0,1, \dots, \infty$$

Equation 55. The equation for evaluating the stability of the system

This equation is very complex to solve, so the recommended way (Mazenc & Niculescu, 2001) to solve this stability problem is, to begin with, the characteristic equation of the system using the following form.

$$\det(sI - A - B * e^{-\tau s}) = 0$$

Equation 56. The characteristic equation of the system

And with Rekasius's definition, the substitution is applied (Olgac & Sipahi, 1995).

$$e^{-\tau s} = \frac{1 - Ts}{1 + Ts}$$

Equation 57. Transfer function

Expanding this term and applying the Routh Hurwitz the values of T can be found, to get an accurate set of T values, but the imaginary values, and the values that satisfy the necessary condition and the additional condition in (Cavdaroglu & Olgac, 2009). With the T values, the next step is to calculate the delay value τ using the following Equation (Cavdaroglu & Olgac, 2009).

$$\tau = \frac{2}{\omega}\left[\tan^{-1}(\omega T) \mp l\pi\right] \quad l = 0,1,2 \dots$$

Equation 58. The equation to convert the value of T in a real delay

Where ω is the natural frequency of the value of T, and l can take any value, but the closest's values to zero are recommended (Cavdaroglu & Olgac, 2009).

With the delay values where a change of the stability appears, is necessary to apply the root tendency to determine if the delay value makes a stable or unstable system.

6.10 Delay compensation control techniques

With the most common stability criteria, the next step was to do short research of the most common method to control delayed systems.

6.10.1 Classical Linear Design

To tune up a classical linear controller in a delayed system, several methods have been developed. These methods can tune up control laws like PID, LQR, and their variances. These laws are the most common in the industrial environment, where delays are a common issue.

One example of this method is observed in (Lee et al., 2000)that works with a classical PID structure and allows to identify of the gains based on the parameters of the model. This method is used for FODUP (first-order delayed unstable process) and SODUP (second-order delayed unstable process), the general structures of the systems are the following:

$$\text{FODUP: } G(s) = \frac{Ke^{-\theta s}}{\tau s - 1}$$

Equation 59. First-order delayed the unstable process

$$\text{SODUP: } G(s) = \frac{Ke^{-\theta s}}{(\tau s - 1)(as + 1)}$$

Equation 60. Second-order delayed the unstable process

After the mathematical process presented in (Lee et al., 2000) the following general structure of the controller is deduced.

$$G_c(s) = K_c\left(1 + \frac{1}{\tau_I s} + \tau_D s\right)$$

Equation 61. The general structure of the controller

Where:

- $K_c = f'(0)$
- $\tau_I = f'(0)/f\ (0)$
- $\tau_I = f''(0)/2f'\ (0)$
- $\tau_I \geq 0; \tau_D \geq 0$

6.10.2 Dead Time Compensation

The dead time compensation is a highly used type controller that cancels the effect of the dead time in a closed-loop system, allowing the controller's design can be achieved using the classical procedure. The DTC (Deadtime compensation) has many variants depending on the study case (Albertos & Garcia, 2007).

The most basic variant of the DTC is the Smith Predictor, This predictor has the following structure, represented by figure 19.

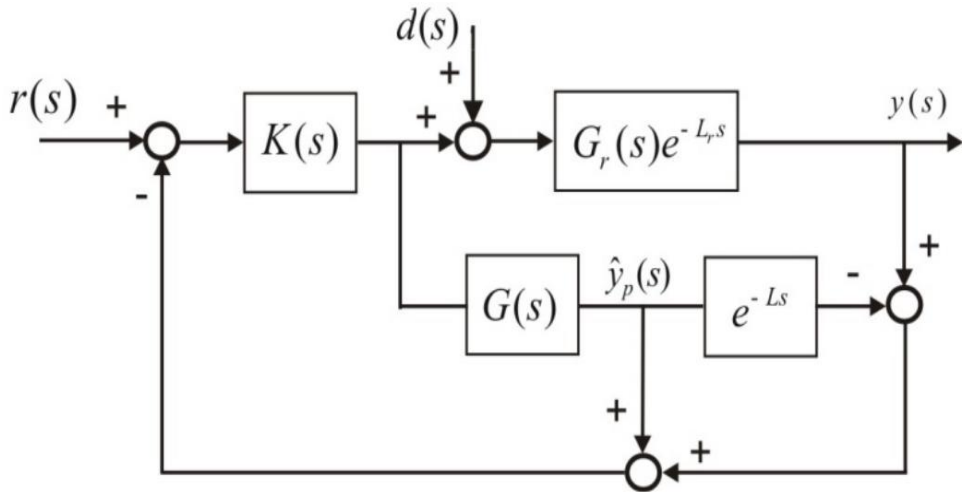

Figure 19. Control Loop of the Smith predictor [n4]

Applying Block's Algebra and considering there are no uncertainties in the model, the following expression is found (Matausek & Micic, 1999).

$$y(s) = \frac{K(s)G(s)e^{-Ls}}{1 + K(s)G(s)e^{-Ls}}\, r(s) + \left(1 - \frac{K(s)G(s)e^{-Ls}}{1 + K(s)G(s)e^{-Ls}}\right) G(s)e^{-Ls}d(s)$$

Equation 62. The output of the Smith predictor [n4]

As can be observed for this structure if the plant has an unstable pole the final system will be unstable and if also the system has an integrator the steady-state error will be different from zero.

To solve the problem many structures were formulated like the one is proposed in (Matausek & Micic, 1999) for systems with integrators that are depicted in the following figure 20.

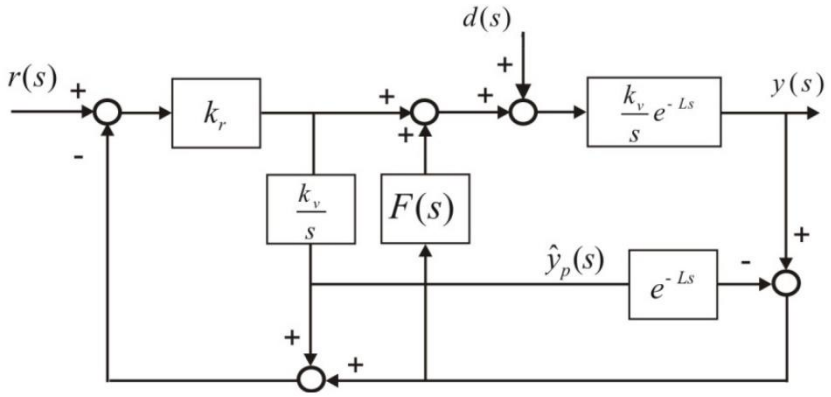

Figure 20. Control Loop of the DTC controller for integrator problems (Matausek & Micic, 1999)

Where

$$F(s) = K_0 \frac{1+T_d S}{1+T_f S}$$

Equation 63. Prefilter used to compensate the delay.

To solve unstable systems the following structure is proposed (Matausek & Micic, 1999). As can be observed this structure increases the degrees of freedom in a high way. For that reason, the design process for this kind of system depends more on the designer.

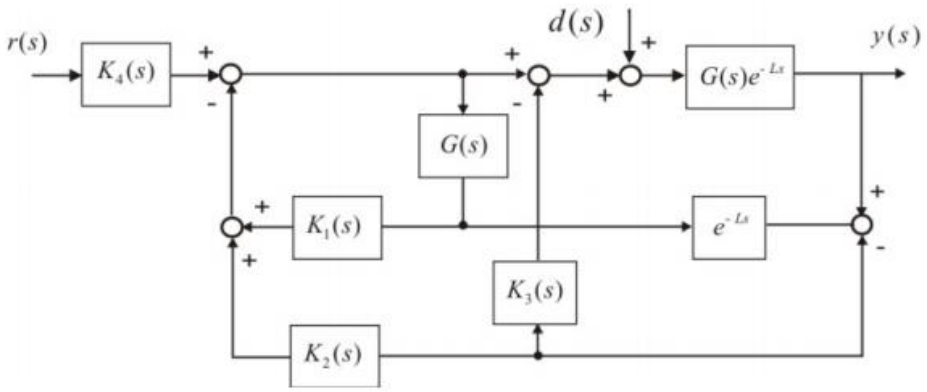

Figure 21. Control Loop of the DTC controller for unstable problems [n5]

6.10.3 Delay scheduling

Delay scheduling is a novel control law that works over a previously designed controller. This characteristic and the fact that is based on the CTCR method allow the implementation in most of the linear controllers (Cavdaroglu & Olgac, 2009).

The main structure of the delay schedule is depicted in the following figure.

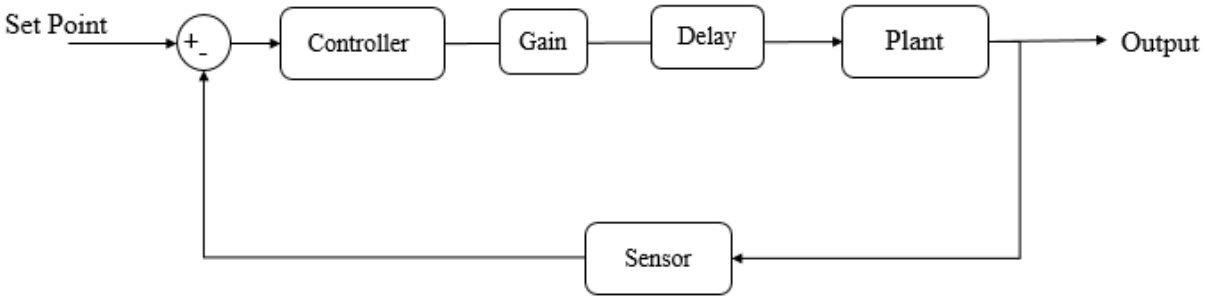

Figure 22. The main structure for delay scheduling control (Cavdaroglu & Olgac, 2009) (Zhang & Tarn, 2002)

The purpose of the delay schedule is to get the gain and the possibility to add an extra delay to get better performance of the closed-loop system.

The procedure to tune a controller with a delay scheduling method is the following:

- Tune the controller assuming a model with no delay
- Apply the CTCR paradigm to determine initial the stability pockets
- Iterate the multiple Gains and get the stability map for each gain value
- If a suitable delay can be added to get into a stability pocket with better response

The main advantage of Delay scheduling is that takes advantage of the CTCR method of identifying more than one stability range of delay, allowing the addition of delay to pass from a pocket of delay to another one (Cavdaroglu & Olgac, 2009). Increasing the possibilities of work with an industrial system with high explicit delays (Zhang & Tarn, 2002).

6.10.4 Sliding Mode Control

The Sliding Mode Control is a robust non-linear control law that can be modified to handle a delayed system adding a predictive state.

SMC controller to determine their stability using the Lyapunov criteria with the Razumikhin method for the delayed system. According to this, the two previously mentioned conditions have to be satisfied with the system to be stable (Roh & Oh, 1999).

The delay system with uncertainties assumed for this SMC design is the following (Roh & Oh, 1999).

$$\dot{x}(t) = Ax(t) + Bu(t-\tau) + f_0(x(t),t) + f_1(x(t-\tau),t)$$

Equation 64. Delay system with uncertain for SMC

To tune the SMC for this case it is necessary to define a predictor (predictive state) (Roh & Oh, 1999).

$$\bar{x}(t) = e^{A\tau}x(t) + \int_{-\tau}^{0} e^{-A\theta} + Bu(t+\theta)d\theta$$

Equation 65. Predictor to tune SMC

The sliding surface defined is the following:

$$\sigma(\bar{x}) = S\bar{x} = 0$$

Equation 66. Sliding surface

After defining the surface the next step is to define the control law that for this case is the following (Roh & Oh, 1999).

$$u(t) = u_{eq} + u_N$$

Equation 67. Control equation for SMC

Where u_{eq} is control action for the nominal system, and u_N is the control action to suppress the uncertainties. The next step is to derivate σ and get u_{eq} getting the following result (Roh & Oh, 1999).

$$u_{eq} = -[SB]^{-1}SA\left[e^{A\tau}x(t) + \int_{-\tau}^{0} e^{-A\theta} + Bu(t+\theta)d\theta\right]$$

$$u_{eq} = -[SB]^{-1}SA\bar{x}$$

Equation 68. Control action of the nominal system

And with the nominal control action, the final step is necessary to find the control action u_N that ensures the tracking of the trajectory (Roh & Oh, 1999).

$$u_N = \begin{cases} -\dfrac{(SB)^{-1}\sigma S e^{A\tau}B}{\|\sigma\|}\hat{\delta}(x,t) & if\ \|\sigma\| \neq 0 \\ 0 & otherwise \end{cases}$$

Equation 69. Control action to suppress uncertainties

7. Methodology

The project development will be divided into five stages with their corresponding activities. The stages will be explained in this section.

7.1 Bibliography research

This stage is the reading process for the articles and books with relevance to the topic.

7.2 Mathematical Modeling of the plant

In this stage, the prototype and the mathematical prototype are defined. And the mathematical model has defined the activities of this stage are the following:

- Identify the failures in the current Pendubot and fix it
- Select the most suitable equations to describe the motion of the Pendubot
- Get the values of the physical properties of the prototype using a gray box method.
- Perform the Best Fit Test to get the closest mathematical model.

7.3 Implementation of the controllers without delay

In this stage with the real prototype and the model, the control laws will be tuned and implemented in the Pendubot:

- Program the Pendubot to read sensor and control actuators using Simulink.
- Using the mathematical model to tune the three control laws
- Implement the three controllers in Simulink and the Pendubot
- Assess the behavior of the controllers

7.4 Application of the “Delay Scheduling” to the control LAWs

In this stage with the tuned controlled the “Delay scheduling” will be applied to improve the performance of the controllers:

- Extract the possible delay values for each controller using the CTCR paradigm.
- Generate an artificial delay considering the stability range for each controller
- Apply the “Delay scheduling ” method in each controller
- Assess the behavior of the controllers with “Delay scheduling”

7.5 Collect data and publish papers

In this stage, the results obtained in each stage will be compiled and will be published in the corresponding proceedings or journals and the final project document.

8. Schedule

Activities completed	
Uncomplete activities	

Activity	Month															
	1	2	3	4	5	6	7	8	9	10	11	12	13	14	15	16
Bibliography research																
Identify the failures in the current Pendubot																
Select the most suitable equations																
Get the values of the physical properties																
Perform a best fit test																
Program the Pendubot																
Tune controllers																
Implement Controllers																
Extract the possible delay values																
Generate an artificial delay																
Apply the "Delay scheduling" method																
Asses the behavior of the controllers																
Collect data and publish papers																

Table 2. Schedule of the project.

9. Prototype

The real prototype is a previously built Pendubot in the laboratory of dynamic systems in the Mechanical Engineering School at the Industrial University of Santander.

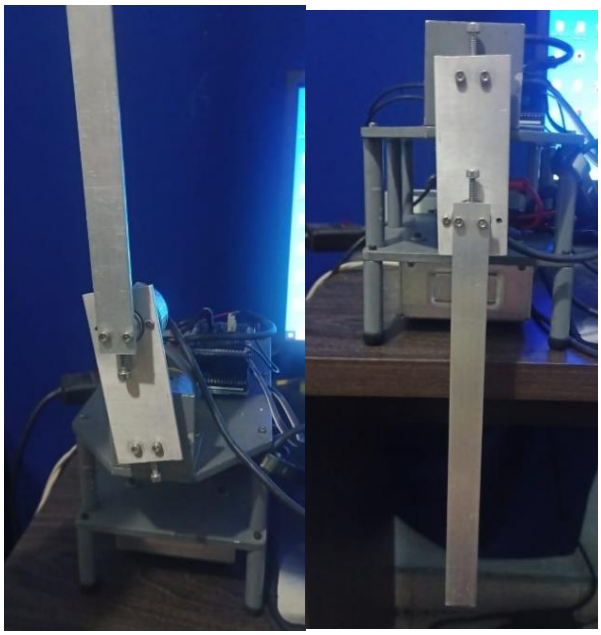

Figure 23. The equilibrium point of Pendubot

Figure 24. The electronic circuit of Pendubot

The Pendubot has the following components:

- Arduino Mega 2560
- Dual motor shield Sparkfun 8 amp
- Handmade Arduino shield for encoder
- PITTMAN loGoc dc motor 24V
- Voltage source 24 V 10 amp
- Encoder with 2500 ppr for each link

This prototype was built as an educative prototype for the laboratory of dynamics system in the Industrial university of Santander. The prototype was designed to satisfy the following characteristics:

- Be modular to be implemented as other control problems
- Use Open source software and hardware
- Be easy to transport

This leads to a prototype suitable for the implementation of advanced control techniques and educational uses.

10. Mathematical Modelling

The mathematical model of a Pendubot is a two-link robot with only one actuator on the first link. The selected actuator was a permanent magnet DC motor. To model the systems the generalized coordinates used can be observed in figure 26.

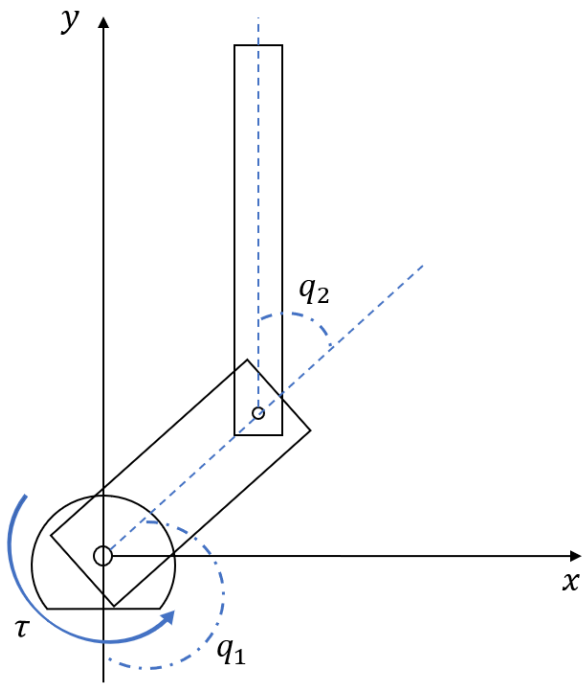

Figure 25. Pendubot DOF diagram

To get a better approximation of the mathematical model the following considerations were applied.

- Bars with a non-centrical mass centroid
- Viscous friction present on each link
- Neglect the effect of the sensors wires
- Consider an ideal DC linear motor

Looking to simplify the modeling process it was divided into two steps, mechanical modeling, and electrical modeling.

10.1 Mechanical modeling

The mechanical model of the Pendubot was carried on using the LaGrange method. This method requires the following steps:

- Potential and kinetic energy definition
- Lagrangian definition
- Derivation of the lagrangian
- Simplification of the equations

According to this, the first step is to find the expression that defines the potential and kinetic energy using the following parameters

Parameter	*Definition*
m_1	Mass of the first link
m_2	Mass of the second link
I_1	Z moment of inertia of the first link
I_2	Z moment of inertia of the second link
l_1	length of the first link
l_{c1}	length of the first link centroid
l_{c2}	length of the second link centroid
q_1	The angle of the first link
q_2	The angle of the second link
b_1	The viscous friction coefficient of the first link
b_2	The viscous friction coefficient of the second link
g	The gravity value
τ	The torque applied by the motor

Table 3. Parameters for mechanical modeling

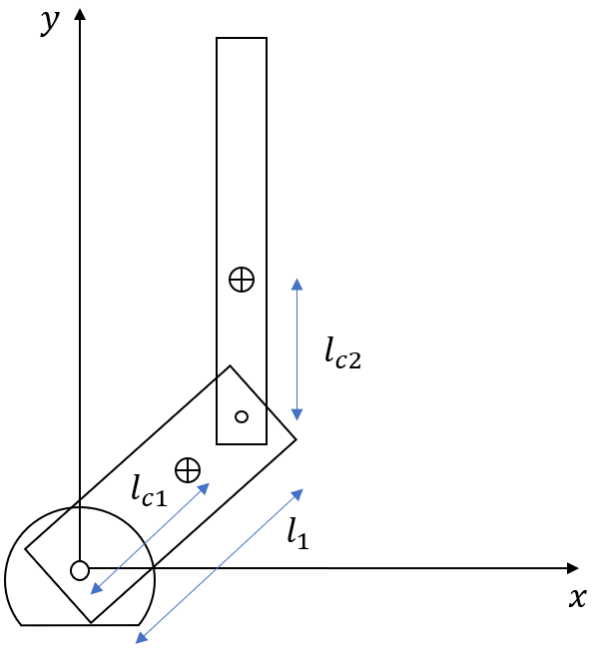

Figure 26. Pendubot parameters diagram

Using the physical definition for each energy the following expressions were obtained.

$$T = \frac{1}{2}m_1((l_{c1}\dot{q}_1)^2) + \frac{1}{2}I_1{\dot{q}_1}^2 + \frac{1}{2}m_2((l_1\dot{q}_1\sin(q_1) + l_{c2}\dot{q}_2\sin(q_2))^2 + (l_1\dot{q}_1\cos(q_1) + l_{c2}\dot{q}_2\cos(q_2))^2) + \frac{1}{2}I_2(\dot{q}_1 + \dot{q}_2)^2$$

Equation 70. Kinetic Energy of the Pendubot

$$U = m_1\ g\ (l_{c1}\cos(q_1)) + m_2\ g\ (l_1\cos(q_1) + l_{c2}\cos(q_2))$$

Equation 71. Potential Energy of the Pendubot

After this the lagrangian was calculated like this:

$$L = T - U$$

Equation 72. LaGrangian equation

$$\begin{aligned} L = \frac{1}{2} m_1((l_{c1}\dot{q_1})^2) + \frac{1}{2} I_1 \dot{q_1}^2 \\ + \frac{1}{2} m_2((l_1\dot{q_1}\sin(q_1) + l_{c2}\dot{q_2}\sin(q_2))^2 \\ + (l_1\dot{q_1}\cos(q_1) + l_{c2}\dot{q_2}\cos(q_2))^2) + \frac{1}{2} I_2(\dot{q_1} + \dot{q_2})^2 \\ - m_1\, g\, (l_{c1}\cos(q_1)) + m_2\, g\, (l_1\cos(q_1) + l_{c2}\cos(q_2)) \end{aligned}$$

Equation 73. LaGrangian expression

Replacing this onto the Euler-Lagrange equation it takes the following expression:

$$\frac{d}{dt}\left(\frac{dL}{d\dot{q}}\right) - \left(\frac{dL}{dq}\right) = F$$

Equation 74. Euler-Lagrange Equation

Assuming the following generalized forces vector:

$$F = \begin{bmatrix} \tau - b_1(\dot{q_1}) + b_2(\dot{q_2}) \\ -b_2(\dot{q_2}) \end{bmatrix}$$

Equation 75. Generalized Forces

After the mathematical process and group the terms in matrices the following expression is obtained :

$$M(q)\,\ddot{q} + C(q,\,\dot{q})\,\dot{q} + N(q,\dot{q}) = \tau_m$$

$$M(q) = \begin{bmatrix} \theta_1 + \theta_2 + 2\theta_3 cos\,(q_2) & \theta_2 + 2\theta_3 cos\,(q_2) \\ \theta_2 + 2\theta_3 cos\,(q_2) & \theta_2 \end{bmatrix}$$

Equation 76. Inertials terms matrix

$$C(q,\, \dot{q}) = \begin{bmatrix} -\theta_3 sin\,(q_2)\dot{q}_2 & -\theta_3 sin\,(q_2)(\dot{q}_2 + \dot{q}_1) \\ \theta_3 sin\,(q_2)(\dot{q}_2) & 0 \end{bmatrix}$$

Equation 77. Coriolis terms matrix

$$N(q,\, \dot{q}) = \begin{bmatrix} \theta_3 g cos(q_1) + \theta_3 g cos(q_1 + q_2) + b_1 q_1 - \dot{b}_2(\dot{q}_2) \\ \theta_5 g cos(q_1 + q_2) + b_2 \dot{q}_2 \end{bmatrix}$$

Equation 78. Non conservative and gravity matrix

$$\theta = \begin{bmatrix} \theta_1 \\ \theta_2 \\ \theta_3 \\ \theta_4 \\ \theta_5 \end{bmatrix} = \begin{bmatrix} m_1 {l_{c1}}^2 + m_2 {l_1}^2 + I_1 \\ m_2 {l_{c2}}^2 + I_2 \\ m_2 l_1 l_{c2} \\ m_1 l_{c1} + m_2 l_1 \\ m_2 l_{c2} \end{bmatrix}$$

Equation 79. Replaced terms matrix

10.2 Electrical modeling

The Pendubot has a DC permanent magnet motor to apply torque to the first link the diagram of this kind of motor is the following:

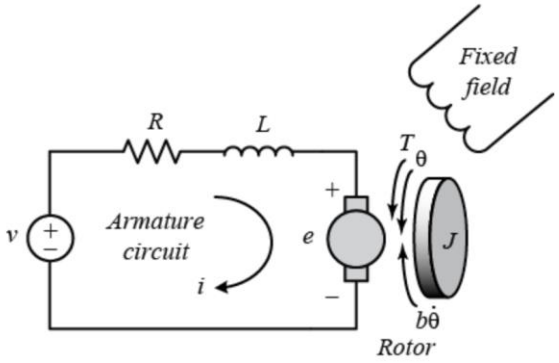

Figure 27. Diagram of the DC permanent magnet motor (Ogata 2010)

This model had been highly developed and used, for this reason, the equation for this motor adapted to the pendubot model is the following (Ogata 2010):

$$\frac{di}{dt} = \frac{1}{L_m}(-R_m I + V - K_e \dot{q}_1)$$

Equation 80. Current equation for a DC motor

$$\tau_{m1} = (K_t i)$$

Equation 81. Relation between Torque and current

10.3 Parameter tuning

With a properly defined model, the next step is to tune the physical parameters. This was carried on using the grey box method.

The methodology used to find these parameters is the next one:

Figure 28. Methodology for model estimation

The experimental data acquired was a single step of PWM with multiple values on the Motor with a sample time of 20 milliseconds. The range of PWM values is (-255 to 255).

An example of the acquired data is the next figures.

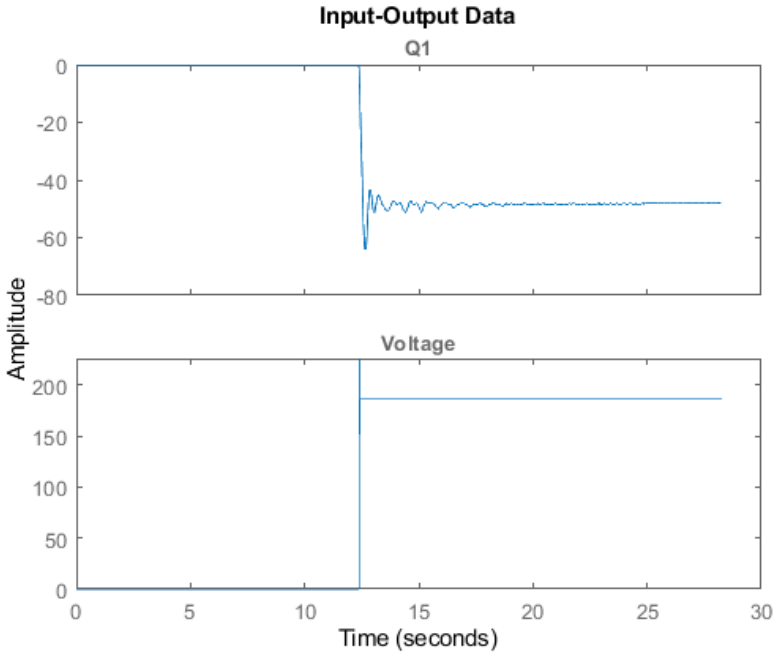

Figure 29. Experimental response of the first link

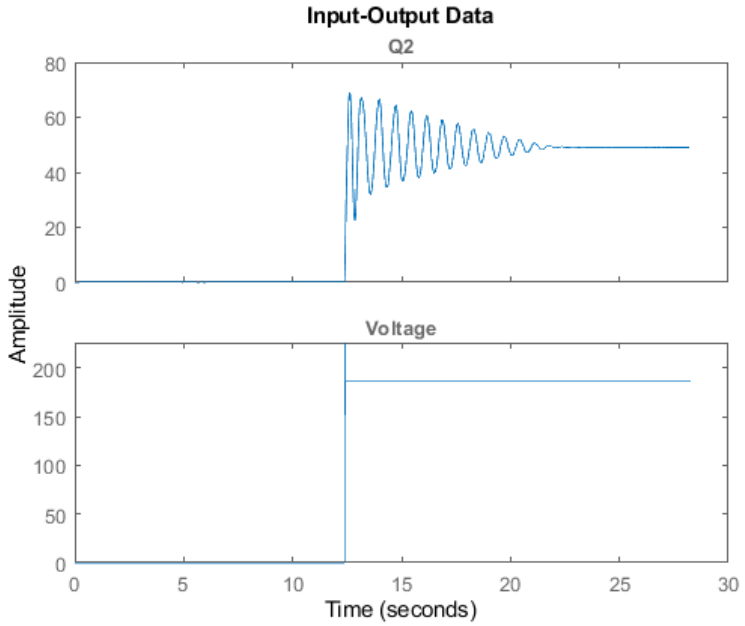

Figure 30. Experimental response of the second link

The grey box method was implemented using the grey box toolbox of MatLab. The following initial parameters were considered:

Parameter	*Initial Value*
θ_1	0.01
θ_2	0.01
θ_3	0.01
θ_4	0.01
θ_5	0.01
R_a	3.94
K_e	20
K_t	2.5
L	0.1
b_1	0.001
b_2	0.001

Table 4. Initial conditions for grey box estimation.

Those values produce the following response on the systems compared to the experimental data:

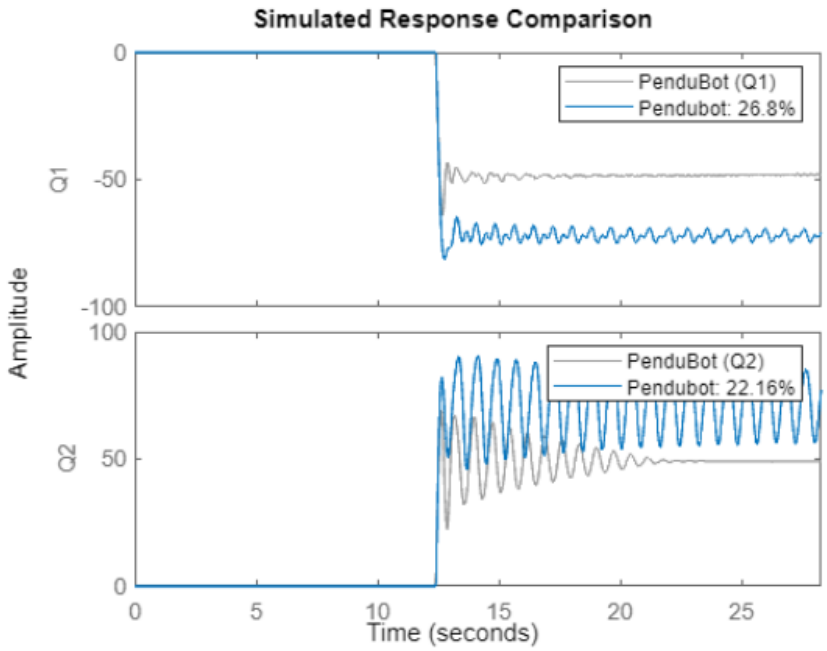

Figure 31. Model behavior for initial parameters

After the tung process using the trust-region reflective newton algorithm with an absolute and relative tolerance of $1x10^{-10}$, the following parameters were obtained.

Parameter	*Value*
θ_1	0.493
θ_2	0.804
θ_3	0.430
θ_4	6.204
θ_5	*7.851*
R_a	3.94
K_e	0.610
K_t	20.637
L	0.1
b_1	0.001
b_2	0.001

Table 5. Final parameters values

These parameters obtain a 93 % of best fit with the initial data as can be observed in the following figure.

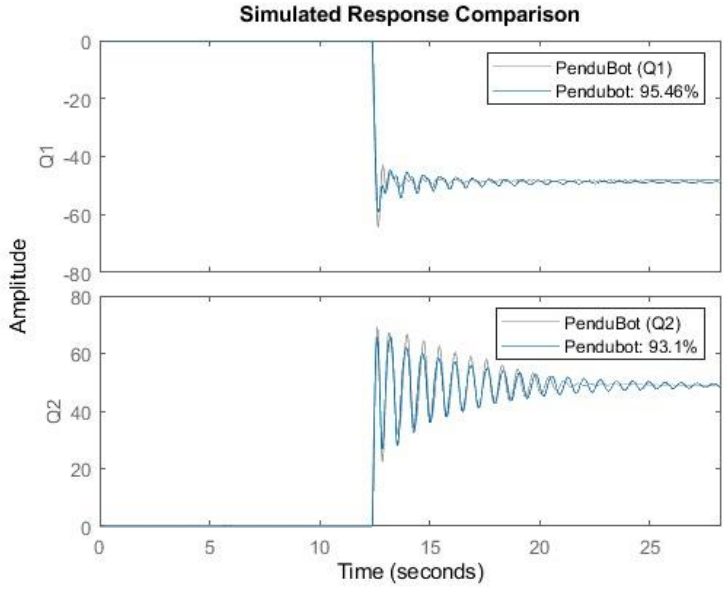

Figure 32. Performance of the model with tune data

Testing the model with different data as validation the following model is obtained:

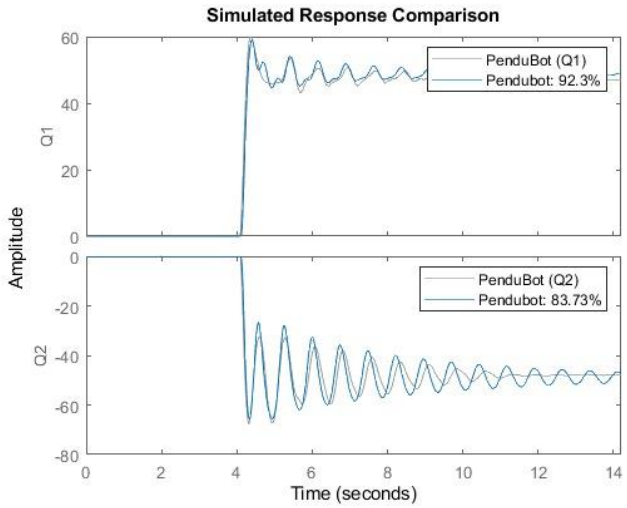

Figure 33. Performance of the model with validation data

This performance shows that the model can predict accurately the behavior of the real prototype.

10.4 Lineal model

Despite the non-linear model being well-tuned, to tune the controllers it is required a linear model to apply the design techniques and the delay scheduling.

To get the linear model the Taylor series method is used to obtain the following A, B, C, and D matrix assuming the equilibrium point of $q_1 = \pi$ and $q_2 = 0$.

$$B = \begin{bmatrix} 0 \\ 0 \\ 0 \\ 0 \\ -0.4706 \end{bmatrix}$$

Equation 82.B matrix of the linear system

$$C = \begin{bmatrix} 0 & 0 & 1 & 0 & 0 \\ 0 & 0 & 0 & 1 & 0 \end{bmatrix}$$

Equation 83. C matrix of the linear system

$$D = \begin{bmatrix} 0 \\ 0 \end{bmatrix}$$

Equation 84.D matrix of the linear system

The step response of this system is unstable which makes sense to the nonlinear model on this equilibrium point as is shown in the next figure.

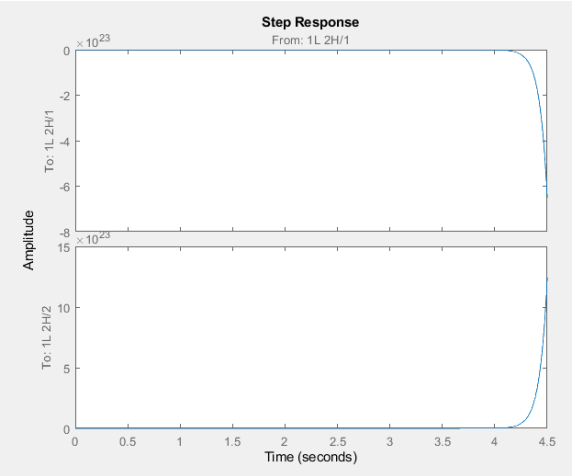

Figure 34. Step response of the linear system

11. Controllers design

Because the CTCR and the delay scheduling method require a non-linear continuous model, all the controllers had to be designed in this form, and in the implementation step, it can be discretized.

11.1 PID design

Because the equilibrium of the second link only can be obtained when the adding of the two angles is equal to π for this reason the following structure was implemented to control the system:

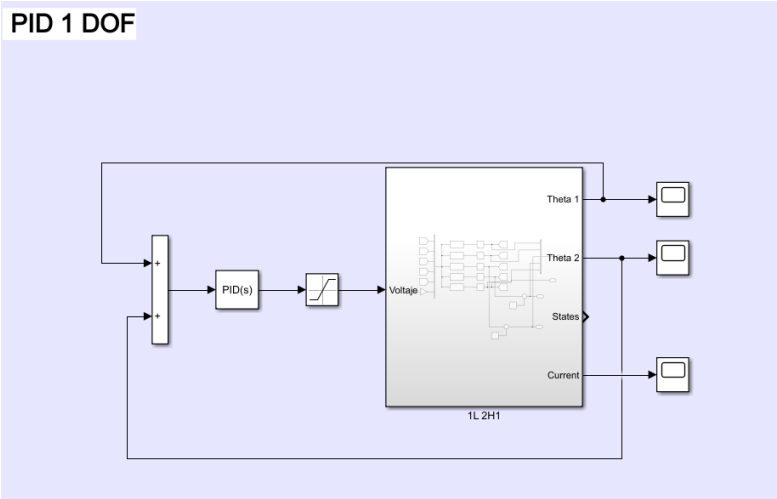

Figure 35. One DOF PID control structure

After the tuning process the following controller constants were obtained:

Constant	*Value*
K_p	-38000
K_i	-67750
K_d	-4745
N	35000

Table 6. One DOF PID constants

The obtaining response to an initial state perturbation is the following:

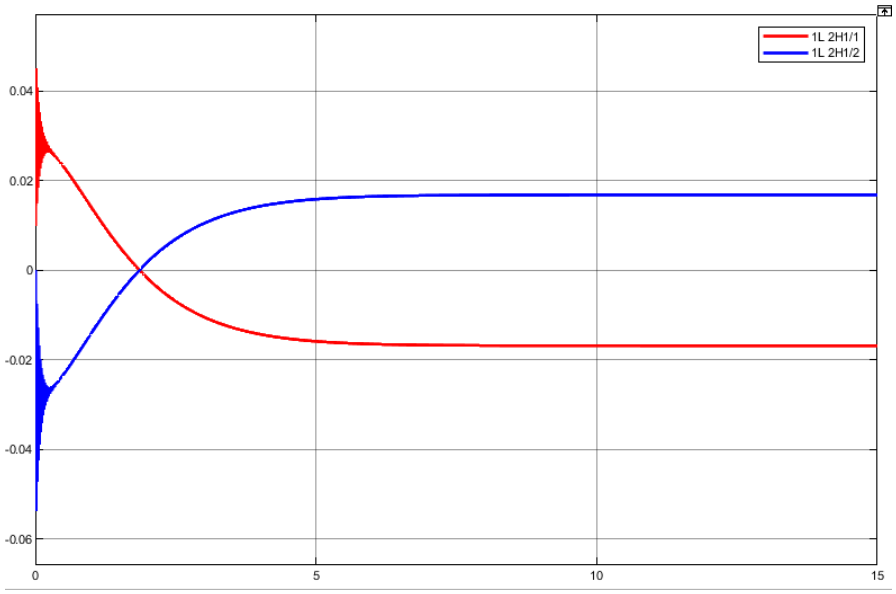

Figure 36. Disturbance response of the two links red is first link and blue second link

As can be observed the final value of the angular position for each link is non-zero. And also was observed several chattering in the initial response of the system for this reason a second PID was tuned. This new PID is a 2 DOF controller using the following structure.

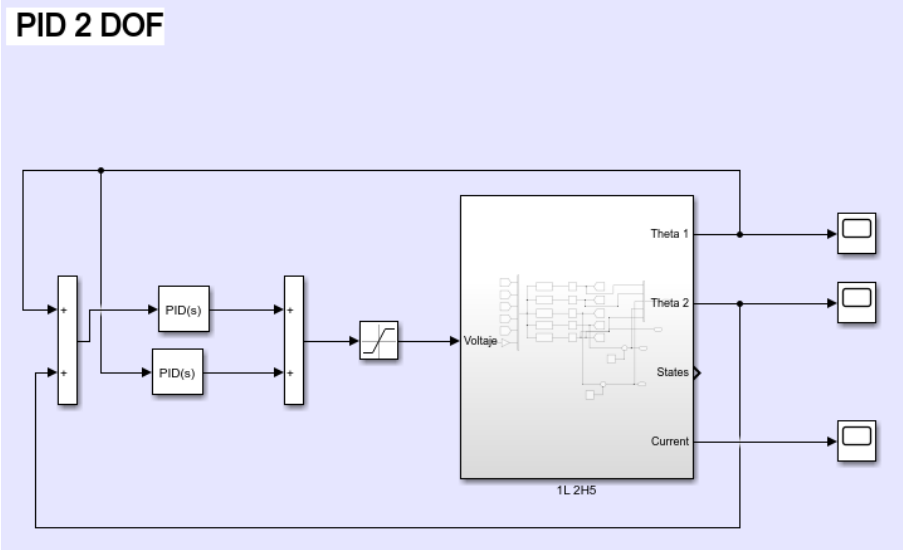

Figure 37. Two DOF PID control structure

This structure was tuned also using auto tune algorithms obtaining an improved response, and their constants are the following.

Constant	*Value*
K_{p1}	-38000
K_{i1}	-67750
K_{d1}	-4745
N_1	35000
K_{p2}	-833.299
K_{i2}	-503.904
K_{d2}	-307.229
N_2	10.884

Table 7. Two DOF PID constants

The disturbance response of this PID control leads the system to the equilibrium point and reduces the chattering in the initial seconds.

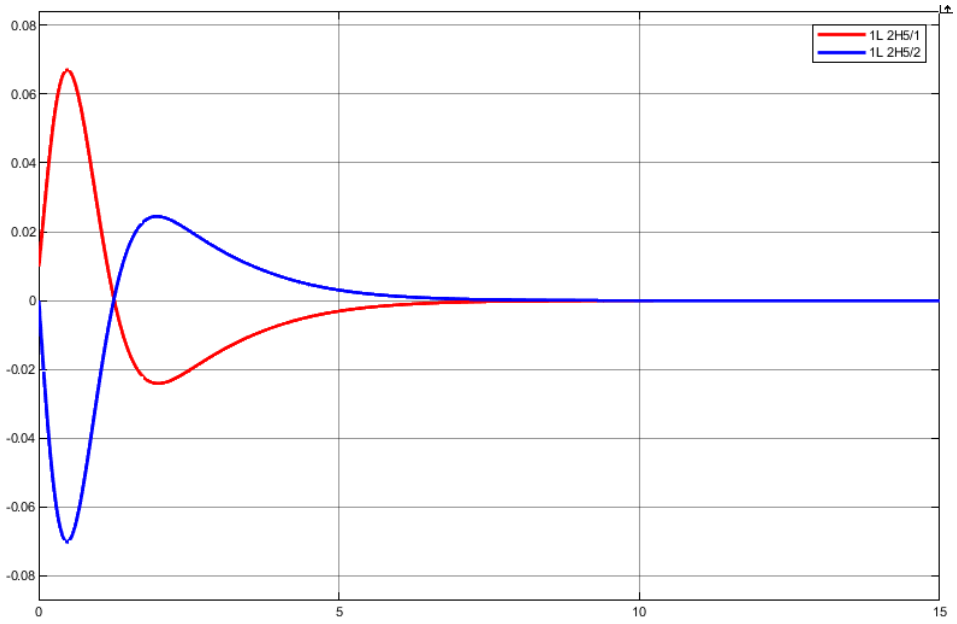

Figure 38. Disturbance response of the 2 DOF PID

11.2 LQG design

The LQG controller is a mixture of an LQR controller with a Kalman estimator. For this reason, the first step is to design the LQR controller.

To apply a state-space controller it is required to determine the controllability of the system. For this reason, the controllability matrix was calculated by obtaining the following matrix.

$$Mc = 1x\ 10^{6}\begin{bmatrix} 0 & 0 & 0.0015 & -0.0527 & 1.5039 \\ 0 & 0.0001 & -0.0022 & 0.0824 & -2.3678 \\ 0 & 0 & 0.0000 & 0.0015 & -0.0527 \\ 0 & 0 & 0.0001 & -0.0022 & 0.0824 \\ 0 & 0 & -0.0005 & 0.0142 & -0.2965 \end{bmatrix}$$

Equation 85. Values of the controllability matrix

Fiding the rank of the controllability matrix it was observed a rank of 5 which means that the system can control all the states. After this, it is required to define the Q and R matrix according to the considered limitations of the real system obtaining the following values.

$$Q = \begin{bmatrix} 100 & 0 & 0 & 0 & 0 \\ 0 & 100 & 0 & 0 & 0 \\ 0 & 0 & 100 & 0 & 0 \\ 0 & 0 & 0 & 100 & 0 \\ 0 & 0 & 0 & 0 & 1 \end{bmatrix}$$

Equation 86. Q matrix for the LQR design

$$R = [0.001]$$

Equation 87. R matrix for the LQR design

Solving the Ricatti equation it was obtained the following gains to the controller.

$$K = 1x\ 10^{4}\begin{bmatrix} 0.2959 \\ 0.2367 \\ 1.9867 \\ 2.0772 \\ -0.0399 \end{bmatrix}$$

Equation 88. Values of gains of the controller

The closed-loop poles of the system are the following:

$$Poles = 1x\ 10^2 \begin{bmatrix} -0.0116 \\ -0.0760 + 0.0080\ i \\ -0.0760 - 0.0080\ i \\ -1.0540 + 1.0165\ i \\ -1.0540 - 1.0165\ i \end{bmatrix}$$

Equation 89. The closed-loop poles of the system

As can be observed the all the real part of the poles is negative which mean that system is fully stable. Implementing the system in Simulink the following structure is applied.

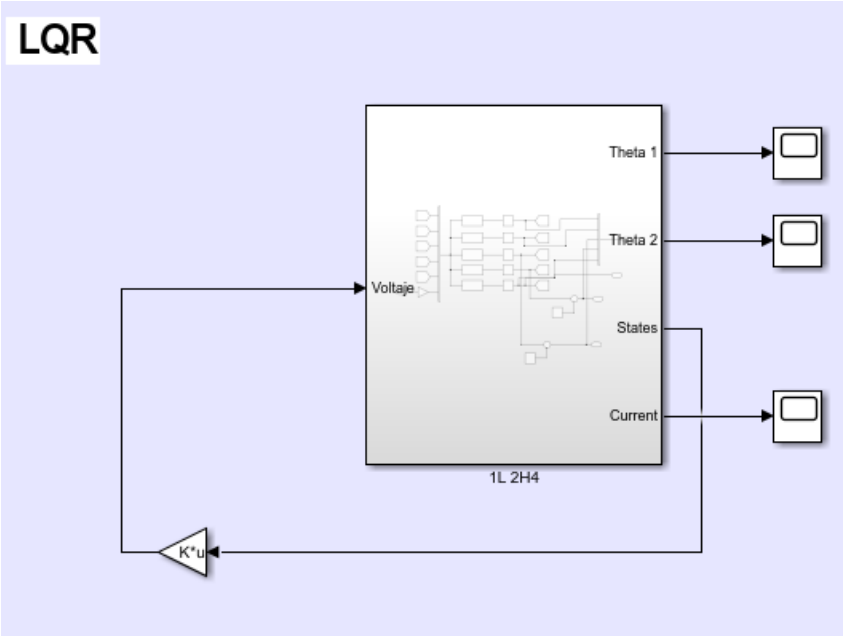

Figure 39. LQR implementation in Simulink

The response of the system with a disturbance of 0.1 [rad] is smooth with no chattering and leads the angles of the links to the equilibrium point.

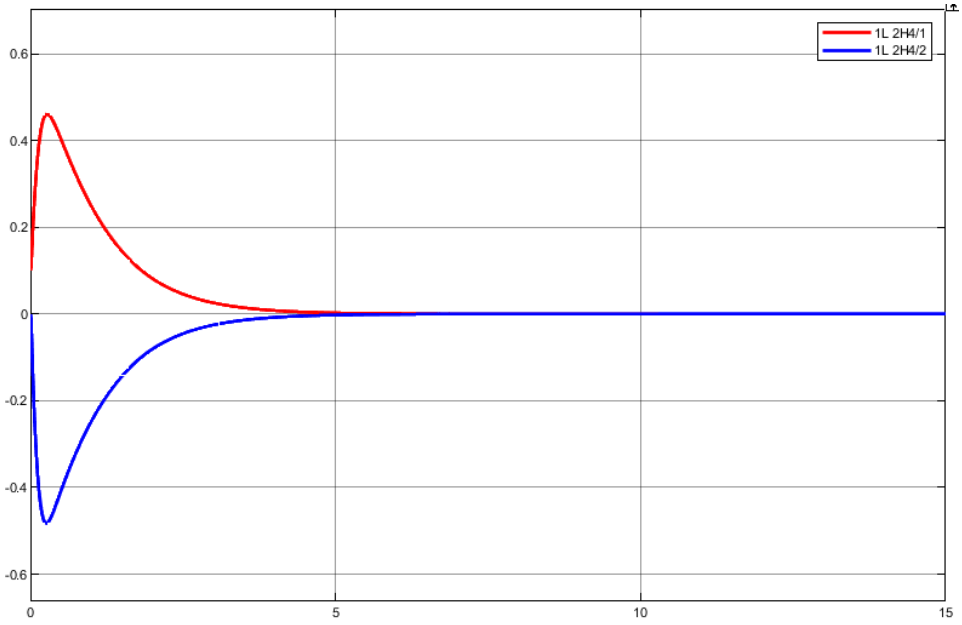

Figure 40. LQR response with disturbance on the first link

After the tuning process of the LQR controller, the next step is to build the Kalman estimator.

To tune an estimator the first step is to find the observability of the system for that reason the observability matrix is calculated:

$$Mob = 1x\ 10^{5}\begin{bmatrix} 0 & 0 & 0.0001 & 0 & 0 \\ 0 & 0.0001 & 0 & 0 & 0 \\ -0.0022 & 0 & 0.0017 & -0.0006 & 0.0008 \\ & -0.0006 & -0.0001 & 0.0001 & -0.0310 \\ 0.1548 & 0 & -0.2633 & 0.0325 & 1.1198 \end{bmatrix}$$

Equation 90. Values of the observability matrix

The rank of this matrix is 5, which means the system is observable for all the states in the system. That leads to the next step in the Kalman filter design is to select the Q and R matrix that represent the noise level for the sensors and actuators.

$$Qn = [0.0001^2]$$

Equation 91. Noise level for the sensors

$$Rn = \begin{bmatrix} 0.0001^2 & 0 \\ 0 & 0.0001^2 \end{bmatrix}$$

Equation 92. Noise level for the actuators

Calculating the Kalman filter the obtained L matrix that allows the state estimation is the following.

$$Lob = \begin{bmatrix} 184.5546 & -105.3324 \\ -125.1679 & 305.3975 \\ 18.4325 & -5.4177 \\ -5.4177 & 24.1131 \\ -18.4177 & 9.4479 \end{bmatrix}$$

Equation 93. Values of the state estimation

With the tuned Kalman filter, the estimator and the controller can be mixed in one state-space system using the following expression.

$$Anew = A - Lob * C - (B - Lob * D) * K$$

Equation 94. A matrix for the LQG controller

$$Bnew = Lob$$

Equation 95. B matrix for the LQG controller

$$Cnew = -K$$

Equation 96. C matrix for the LQG controller

$$Dnew = 0$$

Equation 97. D matrix for the LQG controller

Applying this system on Simulink the following diagram is obtained.

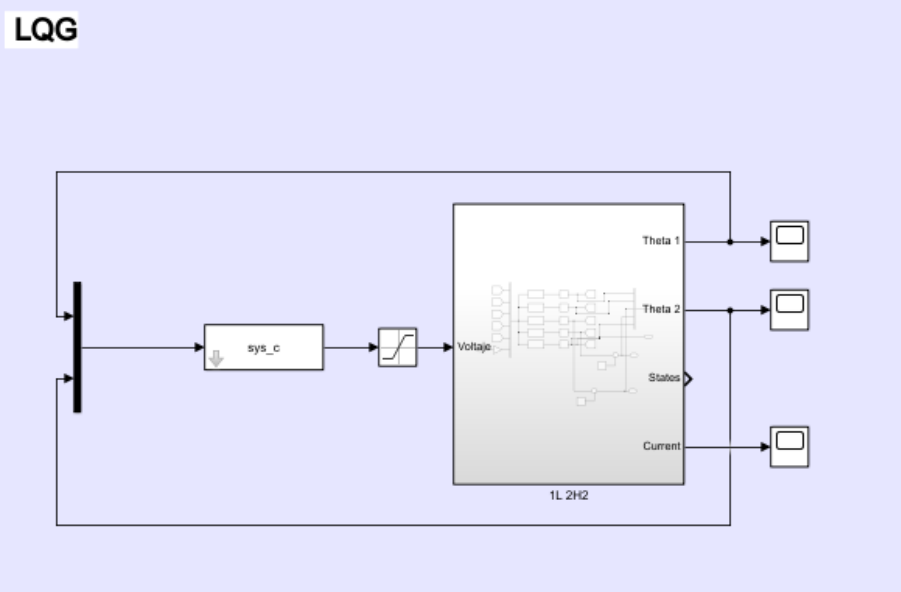

Figure 41. LQG controller implemented in Simulink

Testing the performance of the LQG against angle perturbation controllers generates the following results.

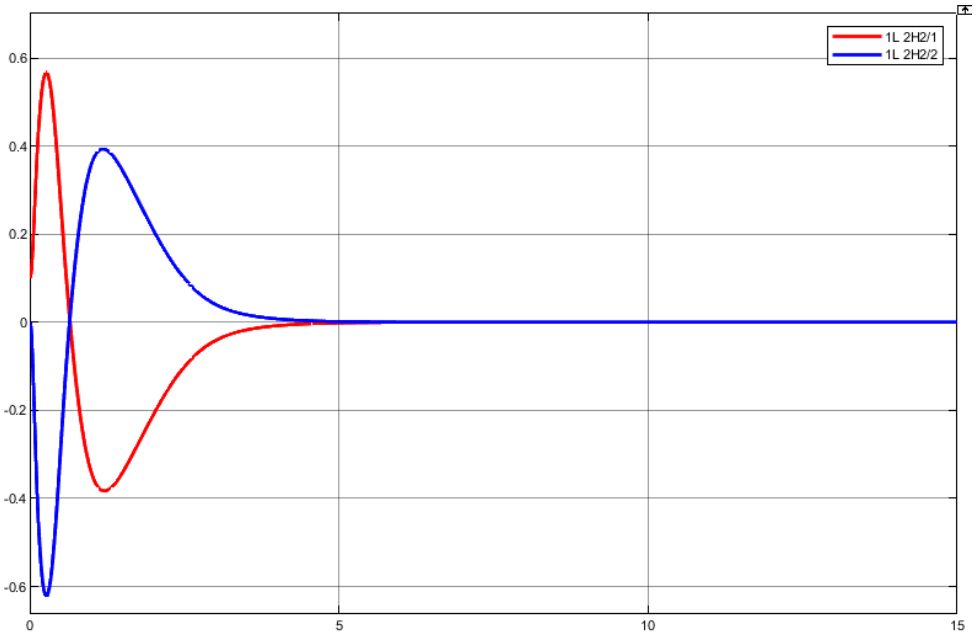

Figure 42. LQG response against angle perturbation

11.3 H∞ controller design

Looking for tuning a controller with a balance between performance and robustness is was applied the mixed-sensitivity loop shaping algorithm. This algorithm uses three weighting sensitivity functions to synthesize the controller.

After the tuning process, the following parameters for the three weightings (W_1, W_2, W_3) functions were selected.

Parameter	*Value*
$Dc\ gain\ for\ W_1$	1
$high\ frequency\ for\ W_1$	0.01
$target\ magnitude\ for\ W_1$	0.1
$frequency\ for\ W_1$	1
$Dc\ gain\ for\ W_2$	0.3
$high\ frequency\ for\ W_2$	0.4
$target\ magnitude\ for\ W_2$	0.32
$frequency\ for\ W_2$	32
$Dc\ gain\ for\ W_3$	0.01
$high\ frequency\ for\ W_3$	1
$target\ magnitude\ for\ W_3$	0.1
$frequency\ for\ W_3$	1

Table 8. Weighting functions parameters

Plotting the bode diagram of the weighting generates the following diagram:

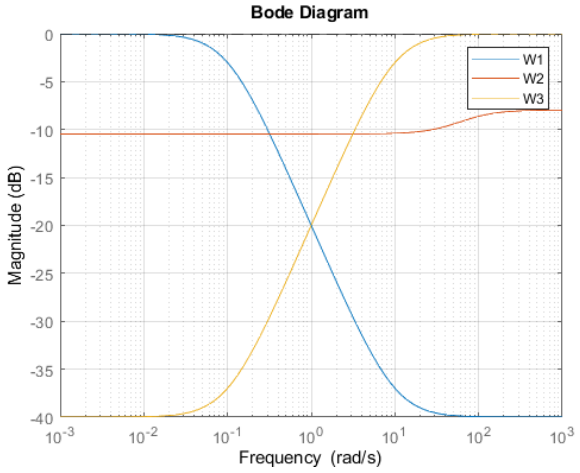

Figure 43. Bode diagram of the weighting functions

After the tuning process using the mixsyn method produce a controller with order 13. And the feedback response against an angle disturbance produces the following response.

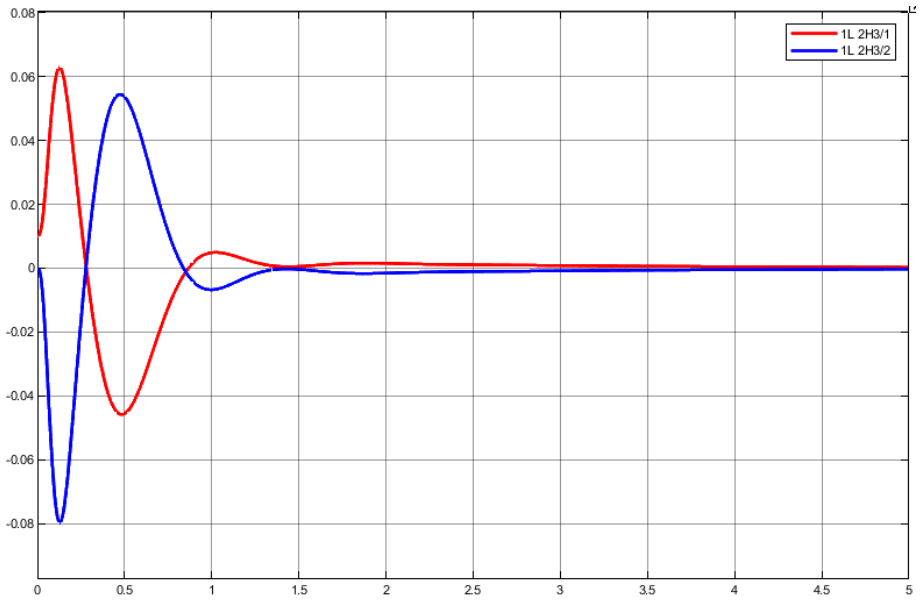

Figure 44. H-infinity response against an angle perturbation

11.4 Controllers comparison

Looking for an objective comparison between the controllers, three parameters were selected to assess the behavior of the strategies. These parameters are the settling time, percentage of overshoot, and the maximum disturbance accepted for the controller.

After multiple tests, the following index of the performance of each controller was obtained.

Parameter	*PID*	*LQG*	$H\infty$
Settling time [Seg]	5.83	3	1.7
Overshoot [%]	623	515	608
Maximum disturbance [rad]	0.03	0.17	0.08

Table 9. The performance index for each controller

The three controllers were plotted to evidence the different performance of each controller monitoring the response of the first link as can be observed in the following figure.

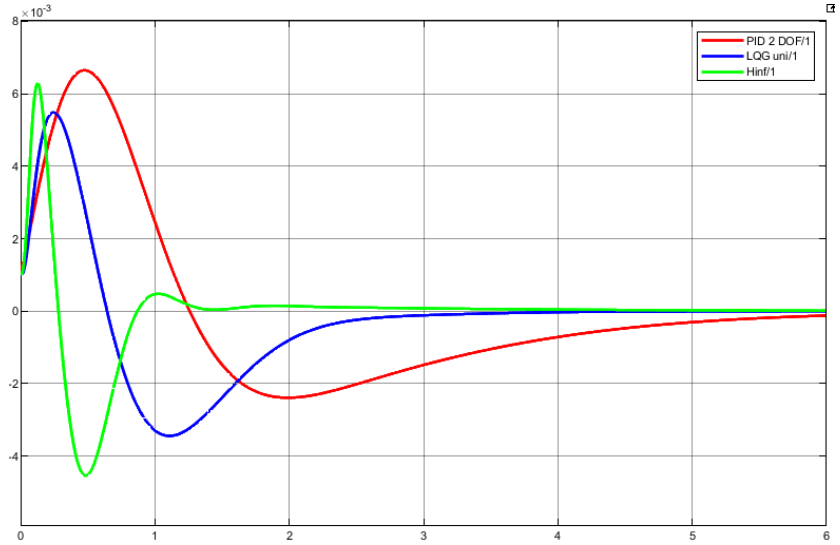

Figure 45. Response of the three controllers against a little perturbation

This analysis evidences the common fact that the PID is the controller with the lower performance. But analyzing the behavior of the LQG is observed that is the most tolerant to angle perturbations, and the H ∞ controller is the fastest one.

12. Delay scheduling

Before the implementation of the controllers to the real prototype it is required to apply the CTCR method to find the delay tolerance for each controller. This is necessary because the real prototype has a minimum sample time of 1 milliseconds. According to this if a controller has a maximum delay tolerance lower than 1 milliseconds, it has to be improved using the delay scheduling before the codification and implementation.

12.1 PID delay scheduling

The first step to use the CTCR paradigm is find the characteristic equation of the closed loop system, and using the Rekasius substitution.

The delay was introduced afther the control action and the alpha gain to improve the controller was setted before the delay according to the following diagram:

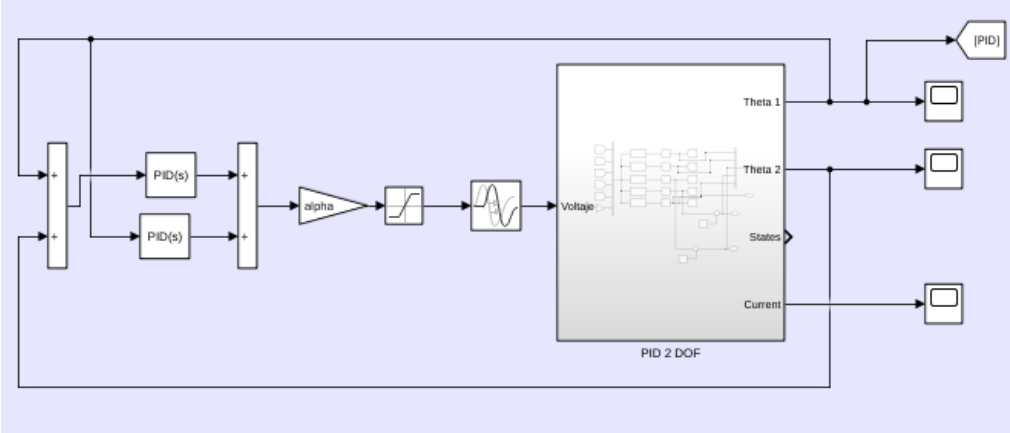

Figure 46 Implementation of the delay and alpha gain

After using the mason theorem an extract the coefficients of the characteristic equation the following expression was obtained to apply the Routh–Hürwitz method, Obtaining the following expression:

$$
\begin{pmatrix}
-1.028e{+}63\,T^6 \\
-3.592e{+}67\,T^6 - 6.171e{+}63\,T^5 \\
-1.414e{+}69\,T^6 - 2.155e{+}68\,T^5 - 1.543e{+}64\,T^4 \\
3.369e{+}72\,T^6\,ds - 2.057e{+}64\,T^3 - 5.388e{+}68\,T^4 - 8.487e{+}69\,T^5 - 1.882e{+}69\,T^6 \\
1.348e{+}73\,T^5\,ds + 2.699e{+}73\,T^6\,ds - 1.543e{+}64\,T^2 - 7.184e{+}68\,T^3 - 2.122e{+}70\,T^4 - 1.129e{+}70\,T^5 + 4.817e{+}71\,T^6 \\
800.0\,T\,(5.192e{+}31\,ds - 6.735e{+}65\,T + 2.106e{+}70\,T^3\,ds + 1.35e{+}71\,T^4\,ds + 6.003e{+}70\,T^5\,ds - 3.536e{+}67\,T^2 - 3.528e{+}67\,T^3 + 3.613e{+}69\,T^4 + 5.479e{+}68\,T^5 - 7.713e{+}60) \\
1.35e{+}74\,T^4\,ds - 2.155e{+}68\,T + 1.921e{+}74\,T^5\,ds - 1.117e{+}71\,T^6\,ds - 2.122e{+}70\,T^2 - 3.764e{+}70\,T^3 + 7.226e{+}72\,T^4 + 2.63e{+}72\,T^5 - 2.477e{+}73\,T^6 - 1.028e{+}63 \\
2.401e{+}74\,T^4\,ds - 1.685e{+}73\,T^2\,ds - 8.487e{+}69\,T - 4.467e{+}71\,T^5\,ds + 1.734e{+}66\,T^6\,ds - 2.823e{+}70\,T^2 + 9.634e{+}72\,T^3 + 6.574e{+}72\,T^4 - 1.486e{+}74\,T^5 - 3.592e{+}67 \\
6.936e{+}66\,T^5\,ds - 1.348e{+}73\,T\,ds - 1.35e{+}74\,T^2\,ds - 5.583e{+}71\,T^4\,ds - 1.129e{+}70\,T + 7.226e{+}72\,T^2 + 8.766e{+}72\,T^3 - 3.716e{+}74\,T^4 - 1.414e{+}69 \\
2.89e{+}72\,T - 3.369e{+}72\,ds - 1.08e{+}74\,T\,ds - 2.401e{+}74\,T^2\,ds + 8.67e{+}66\,T^4\,ds - 4.154e{+}34\,T^5\,ds + 6.574e{+}72\,T^2 - 4.955e{+}74\,T^3 - 1.882e{+}69 \\
2.63e{+}72\,T - 2.699e{+}73\,ds - 1.921e{+}74\,T\,ds + 5.583e{+}71\,T^2\,ds - 3.716e{+}74\,T^2 + 4.817e{+}71 \\
4.467e{+}71\,T\,ds - 4.802e{+}73\,ds - 1.486e{+}74\,T - 8.67e{+}66\,T^2\,ds + 4.383e{+}71 \\
1.117e{+}71\,ds - 6.936e{+}66\,T\,ds - 2.477e{+}73 \\
-1.734e{+}66\,ds
\end{pmatrix}
$$

Figure 47 Characteristic equation coefficients for PID

The system after applying de CTCR paradigm in the initial controller It was obtained a value of 0.34 [ms], for this reason, it was necessary to tune the alpha gain to increase the delay tolerance of the system. After this process, it was observed that the maximum delay value of delay for the PID is 3.51 [ms]. This tuning process makes it possible to implement the controller in the real experiment. The delay scheduling plot obtained can be observed in the following figure.

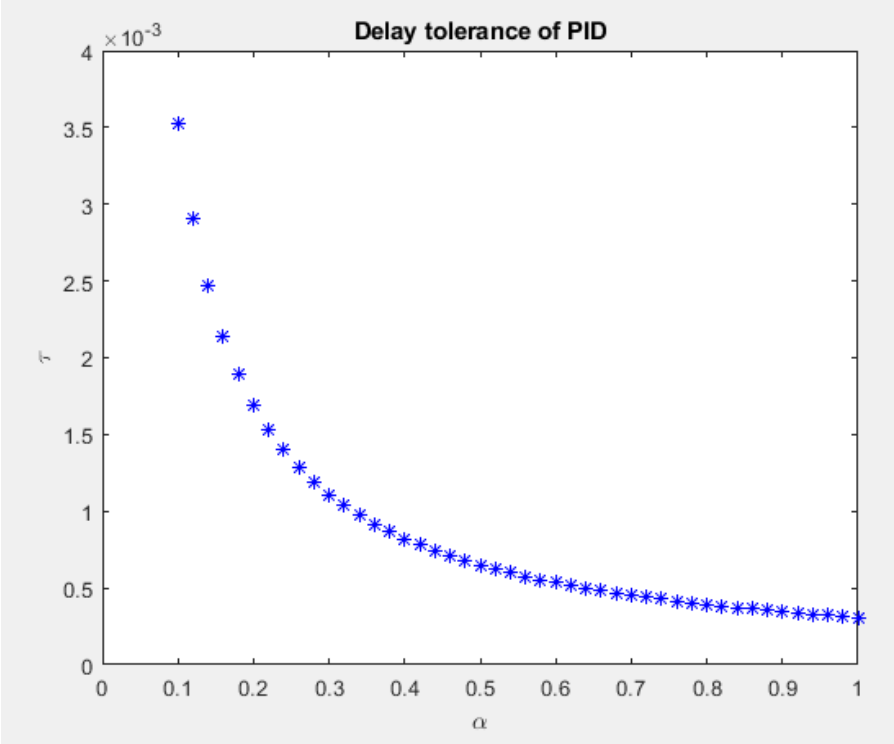

Figure 48 Delay tolerance of the PID

12.2 LQG delay scheduling

For the case of the PID controller, the mason theorem was easily applied because of the controller's response as a transfer function. But for the case of the LQG controller, a general matrix form was applied according to the following equation.

$$Tf_{plant} = C_{plant}\left(S * I - A_{plant}\right)^{-1} * B_{plant} * \frac{1 - Ts}{1 + Ts}$$

$$Tf_{controller} = Ds_{gain}(C_{controller}(S * I - A_{controller})^{-1} * B_{controller} + D_{controller})$$

$$Tf_{sys} = \frac{Tf_{plant} * Tf_{controller}}{1 - Tf_{plant} * Tf_{controller}}$$

This general form allows passing every linear controller in a matrix form where Tf_{sys} could be a vector of transfer function where they keep the same characteristic equation.
Using this method on the LQG controller the next characteristic equation coefficients were obtained.

$$\begin{pmatrix}
2.271e{+}134\,T^6 \\
7.021e{+}136\,T^6 + 1.363e{+}135\,T^5 \\
1.05e{+}139\,T^6 + 4.213e{+}137\,T^5 + 3.407e{+}135\,T^4 \\
6.93e{+}140\,T^6 + 6.299e{+}139\,T^5 + 1.053e{+}138\,T^4 + 4.543e{+}135\,T^3 \\
3.407e{+}135\,T^2 - 6.029e{+}141\,T^6\,\mathrm{ds} + 1.404e{+}138\,T^3 + 1.575e{+}140\,T^4 + 4.158e{+}141\,T^5 + 1.821e{+}142\,T^6 \\
1.0e{+}103\,T\ (1.053e{+}35\,T - 2.411e{+}39\,T^4\,\mathrm{ds} - 4.175e{+}40\,T^5\,\mathrm{ds} + 2.1e{+}37\,T^2 + 1.04e{+}39\,T^3 + 1.092e{+}40\,T^4 + 7.008e{+}39\,T^5 + 1.363e{+}32) \\
4.213e{+}137\,T - 3.014e{+}142\,T^4\,\mathrm{ds} - 1.67e{+}144\,T^5\,\mathrm{ds} - 1.043e{+}145\,T^6\,\mathrm{ds} + 1.575e{+}140\,T^2 + 1.386e{+}142\,T^3 + 2.731e{+}143\,T^4 + 4.205e{+}143\,T^5 - 4.57e{+}144\,T^6 + 2.271e{+}134 \\
6.299e{+}139\,T - 2.088e{+}144\,T^4\,\mathrm{ds} - 4.17e{+}145\,T^5\,\mathrm{ds} - 9.21e{+}145\,T^6\,\mathrm{ds} + 1.04e{+}142\,T^2 + 3.642e{+}143\,T^3 + 1.051e{+}144\,T^4 - 2.742e{+}145\,T^5 - 5.011e{+}145\,T^6 + 7.021e{+}136 \\
4.158e{+}141\,T + 3.014e{+}142\,T^2\,\mathrm{ds} - 5.213e{+}145\,T^4\,\mathrm{ds} - 3.684e{+}146\,T^5\,\mathrm{ds} - 6.654e{+}145\,T^6\,\mathrm{ds} + 2.731e{+}143\,T^2 + 1.402e{+}144\,T^3 - 6.855e{+}145\,T^4 - 3.007e{+}146\,T^5 + 1.049e{+}146\,T^6 + 1.05e{+}139 \\
1.092e{+}143\,T + 2.411e{+}142\,T\,\mathrm{ds} + 2.088e{+}144\,T^2\,\mathrm{ds} - 4.605e{+}146\,T^4\,\mathrm{ds} - 2.662e{+}146\,T^5\,\mathrm{ds} + 2.205e{+}147\,T^6\,\mathrm{ds} + 1.051e{+}144\,T^2 - 9.14e{+}145\,T^3 - 7.517e{+}146\,T^4 + 6.291e{+}146\,T^5 + 2.552e{+}147\,T^6 + 6.93e{+}140 \\
4.205e{+}143\,T + 6.029e{+}141\,\mathrm{ds} + 1.67e{+}144\,T\,\mathrm{ds} + 5.213e{+}145\,T^2\,\mathrm{ds} - 3.327e{+}146\,T^4\,\mathrm{ds} + 8.821e{+}147\,T^5\,\mathrm{ds} + 5.268e{+}147\,T^6\,\mathrm{ds} - 6.855e{+}145\,T^2 - 1.002e{+}147\,T^3 + 1.573e{+}147\,T^4 + 1.531e{+}148\,T^5 + 5.496e{+}147\,T^6 + 1.821e{+}142 \\
4.175e{+}143\,\mathrm{ds} - 2.742e{+}145\,T + 4.17e{+}145\,T\,\mathrm{ds} + 4.605e{+}146\,T^2\,\mathrm{ds} + 1.103e{+}148\,T^4\,\mathrm{ds} + 2.107e{+}148\,T^5\,\mathrm{ds} - 7.517e{+}146\,T^2 + 2.097e{+}147\,T^3 + 3.828e{+}148\,T^4 + 3.298e{+}148\,T^5 + 7.008e{+}142 \\
1.043e{+}145\,\mathrm{ds} - 3.007e{+}146\,T + 3.684e{+}146\,T\,\mathrm{ds} + 3.327e{+}146\,T^2\,\mathrm{ds} + 2.634e{+}148\,T^4\,\mathrm{ds} + 1.573e{+}147\,T^2 + 5.105e{+}148\,T^3 + 8.244e{+}148\,T^4 - 4.57e{+}144 \\
6.291e{+}146\,T + 9.21e{+}145\,\mathrm{ds} + 2.662e{+}146\,T\,\mathrm{ds} - 1.103e{+}148\,T^2\,\mathrm{ds} + 3.828e{+}148\,T^2 + 1.099e{+}149\,T^3 - 5.011e{+}145 \\
1.531e{+}148\,T + 6.654e{+}145\,\mathrm{ds} - 8.821e{+}147\,T\,\mathrm{ds} - 2.634e{+}148\,T^2\,\mathrm{ds} + 8.244e{+}148\,T^2 + 1.049e{+}146 \\
3.298e{+}148\,T - 2.205e{+}147\,\mathrm{ds} - 2.107e{+}148\,T\,\mathrm{ds} + 2.552e{+}147 \\
5.496e{+}147 - 5.268e{+}147\,\mathrm{ds}
\end{pmatrix}$$

Figure 49 characteristic equations coefficients of LQG

Applying the CTCR paradigm and the delay scheduling process was observed that the default delay tolerance is about 17.5 [ms]. After the test on the gain in different ranges, it was observed that in contrast to the PID controller the gain does not increase significantly the tolerance of the controller. This behavior can be observed in the following figure.

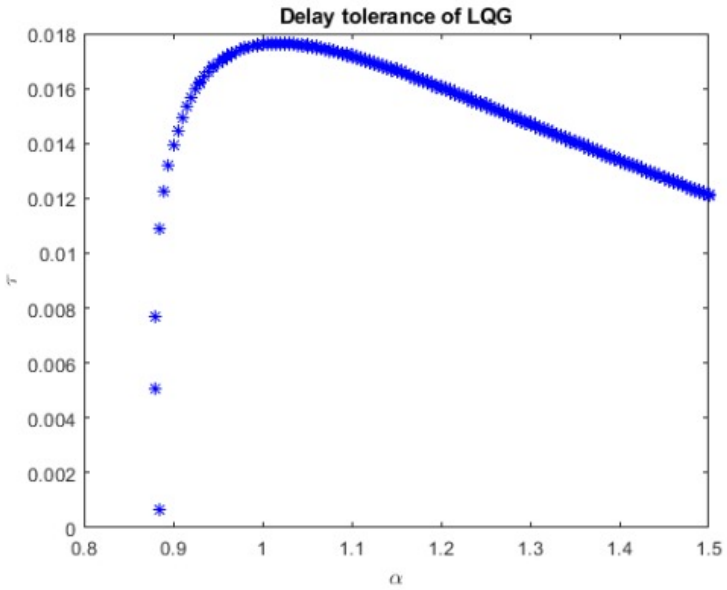

Figure 50 Delay scheduling of the LQG controller

12.3 H∞ delay scheduling

For the case of the H∞ control, an order reduction was applied to reduce the computational time and other issues like the "out of memory" error produced by the long size of symbolic expressions.

After the order reduction process, the same method used on the LQG was implemented obtaining the following characteristic equation coefficients.

$$
\begin{pmatrix}
6.512e{+}239\,T^6 \\
2.679e{+}243\,T^6 + 3.907e{+}240\,T^5 \\
5.338e{+}245\,T^6 + 1.607e{+}244\,T^5 + 9.768e{+}240\,T^4 \\
4.72e{+}247\,T^6 + 3.203e{+}246\,T^5 + 4.018e{+}244\,T^4 + 1.302e{+}241\,T^3 \\
9.768e{+}240\,T^2 - 2.553e{+}248\,T^6\,\mathrm{ds} + 5.358e{+}244\,T^3 + 8.007e{+}246\,T^4 + 2.832e{+}248\,T^5 + 2.155e{+}249\,T^6 \\
2.0e{+}208\,T\ (2.009e{+}36\,T - 5.106e{+}40\,T^4\,\mathrm{ds} - 1.777e{+}42\,T^5\,\mathrm{ds} + 5.338e{+}38\,T^2 + 3.54e{+}40\,T^3 + 6.466e{+}41\,T^4 + 2.142e{+}42\,T^5 + 1.954e{+}32) \\
1.607e{+}244\,T - 1.276e{+}249\,T^4\,\mathrm{ds} - 1.422e{+}251\,T^5\,\mathrm{ds} - 1.7e{+}252\,T^6\,\mathrm{ds} + 8.007e{+}246\,T^2 + 9.441e{+}248\,T^3 + 3.233e{+}250\,T^4 + 2.571e{+}251\,T^5 - 1.151e{+}250\,T^6 + 6.512e{+}239 \\
3.203e{+}246\,T - 1.777e{+}251\,T^4\,\mathrm{ds} - 6.801e{+}252\,T^5\,\mathrm{ds} - 3.661e{+}253\,T^6\,\mathrm{ds} + 7.08e{+}248\,T^2 + 4.311e{+}250\,T^3 + 6.426e{+}251\,T^4 - 6.909e{+}250\,T^5 - 1.226e{+}253\,T^6 + 2.679e{+}243 \\
2.832e{+}248\,T + 1.276e{+}249\,T^2\,\mathrm{ds} - 8.502e{+}252\,T^4\,\mathrm{ds} - 1.465e{+}254\,T^5\,\mathrm{ds} - 3.354e{+}254\,T^6\,\mathrm{ds} + 3.233e{+}250\,T^2 + 8.569e{+}251\,T^3 - 1.727e{+}251\,T^4 - 7.359e{+}253\,T^5 - 1.033e{+}254\,T^6 + 5.338e{+}245 \\
1.293e{+}250\,T + 1.021e{+}249\,T\,\mathrm{ds} + 1.777e{+}251\,T^2\,\mathrm{ds} - 1.831e{+}254\,T^4\,\mathrm{ds} - 1.342e{+}255\,T^5\,\mathrm{ds} - 1.01e{+}255\,T^6\,\mathrm{ds} + 6.426e{+}251\,T^2 - 2.303e{+}251\,T^3 - 1.84e{+}254\,T^4 - 6.199e{+}254\,T^5 + 3.997e{+}254\,T^6 + 4.72e{+}247 \\
2.571e{+}251\,T + 2.553e{+}248\,\mathrm{ds} + 1.422e{+}251\,T\,\mathrm{ds} + 8.502e{+}252\,T^2\,\mathrm{ds} - 1.677e{+}255\,T^4\,\mathrm{ds} - 4.041e{+}255\,T^5\,\mathrm{ds} + 5.386e{+}254\,T^6\,\mathrm{ds} - 1.727e{+}251\,T^2 - 2.453e{+}254\,T^3 - 1.55e{+}255\,T^4 + 2.398e{+}255\,T^5 + 5.576e{+}255\,T^6 + 2.155e{+}249 \\
3.554e{+}250\,\mathrm{ds} - 6.909e{+}250\,T + 6.801e{+}252\,T\,\mathrm{ds} + 1.831e{+}254\,T^2\,\mathrm{ds} - 5.051e{+}255\,T^4\,\mathrm{ds} + 2.154e{+}255\,T^5\,\mathrm{ds} + 6.215e{+}253\,T^6\,\mathrm{ds} - 1.84e{+}254\,T^2 - 2.066e{+}255\,T^3 + 5.995e{+}255\,T^4 + 3.346e{+}256\,T^5 + 8.873e{+}255\,T^6 + 4.284e{+}250 \\
1.7e{+}252\,\mathrm{ds} - 7.359e{+}253\,T + 1.465e{+}254\,T\,\mathrm{ds} + 1.677e{+}255\,T^2\,\mathrm{ds} + 2.693e{+}255\,T^4\,\mathrm{ds} + 2.486e{+}254\,T^5\,\mathrm{ds} - 1.472e{+}251\,T^6\,\mathrm{ds} - 1.55e{+}255\,T^2 + 7.993e{+}255\,T^3 + 8.365e{+}256\,T^4 + 5.324e{+}256\,T^5 + 4.109e{+}255\,T^6 - 1.151e{+}250 \\
3.661e{+}253\,\mathrm{ds} - 6.199e{+}254\,T + 1.342e{+}255\,T\,\mathrm{ds} + 5.051e{+}255\,T^2\,\mathrm{ds} + 3.108e{+}254\,T^4\,\mathrm{ds} - 5.889e{+}251\,T^5\,\mathrm{ds} + 2.286e{+}246\,T^6\,\mathrm{ds} + 5.995e{+}255\,T^2 + 1.115e{+}257\,T^3 + 1.331e{+}257\,T^4 + 2.465e{+}256\,T^5 + 3.277e{+}254\,T^6 - 1.226e{+}253 \\
2.398e{+}255\,T + 3.354e{+}254\,\mathrm{ds} + 4.041e{+}255\,T\,\mathrm{ds} - 2.693e{+}255\,T^2\,\mathrm{ds} - 7.361e{+}251\,T^4\,\mathrm{ds} + 9.145e{+}246\,T^5\,\mathrm{ds} + 8.365e{+}256\,T^2 + 1.775e{+}257\,T^3 + 6.164e{+}256\,T^4 + 1.966e{+}255\,T^5 - 1.033e{+}254 \\
3.346e{+}256\,T + 1.01e{+}255\,\mathrm{ds} - 2.154e{+}255\,T\,\mathrm{ds} - 3.108e{+}254\,T^2\,\mathrm{ds} + 1.143e{+}247\,T^4\,\mathrm{ds} + 1.331e{+}257\,T^2 + 8.218e{+}256\,T^3 + 4.916e{+}255\,T^4 + 3.997e{+}254 \\
5.324e{+}256\,T - 5.386e{+}254\,\mathrm{ds} - 2.486e{+}254\,T\,\mathrm{ds} + 7.361e{+}251\,T^2\,\mathrm{ds} + 6.164e{+}256\,T^2 + 6.554e{+}255\,T^3 + 5.576e{+}255 \\
2.465e{+}256\,T - 6.215e{+}253\,\mathrm{ds} + 5.889e{+}251\,T\,\mathrm{ds} - 1.143e{+}247\,T^2\,\mathrm{ds} + 4.916e{+}255\,T^2 + 8.873e{+}255 \\
1.966e{+}255\,T + 1.472e{+}251\,\mathrm{ds} - 9.145e{+}246\,T\,\mathrm{ds} + 4.109e{+}255 \\
3.277e{+}254 - 2.286e{+}246\,\mathrm{ds}
\end{pmatrix}
$$

Figure 51characteristic equations coefficients of H infinity

This controller was the only one of the three controllers that after the delay scheduling process obtain two pockets. As the LQG controller, the gain does not increase significantly

the delay tolerance. The maximum delay tolerance for this controller is 12.5[ms]. The delay scheduling response of the system is the following.

.

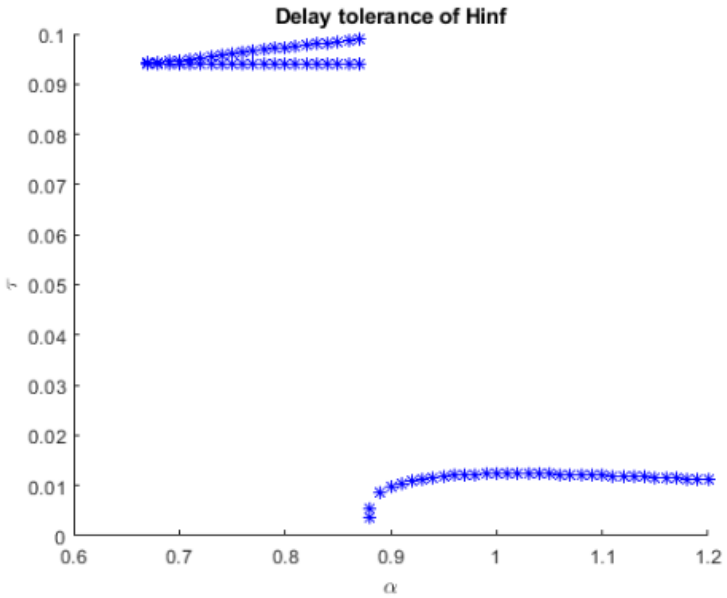

Figure 52 Delay scheduling of H infinity controller

Analyzing the stability pockets it was observed that the pocket with a higher delay value does not stabilize the system. This was discovered by applying the number of unstable roots on that pocket. This shows that the system became more unstable at this point, passing from 4 unstable roots to 8 unstable roots.

13. Experimental implementation

Implementing all the controllers on the real prototype with a sample rate of 1 [kHz] the following response of the controllers were obtained.

For the PID controller, it was observed an extremely aggressive response but it keeps stable, but only with the gain tuned with delay scheduling to its maximum value. The system keeps oscillating between -7 to 7 degrees.

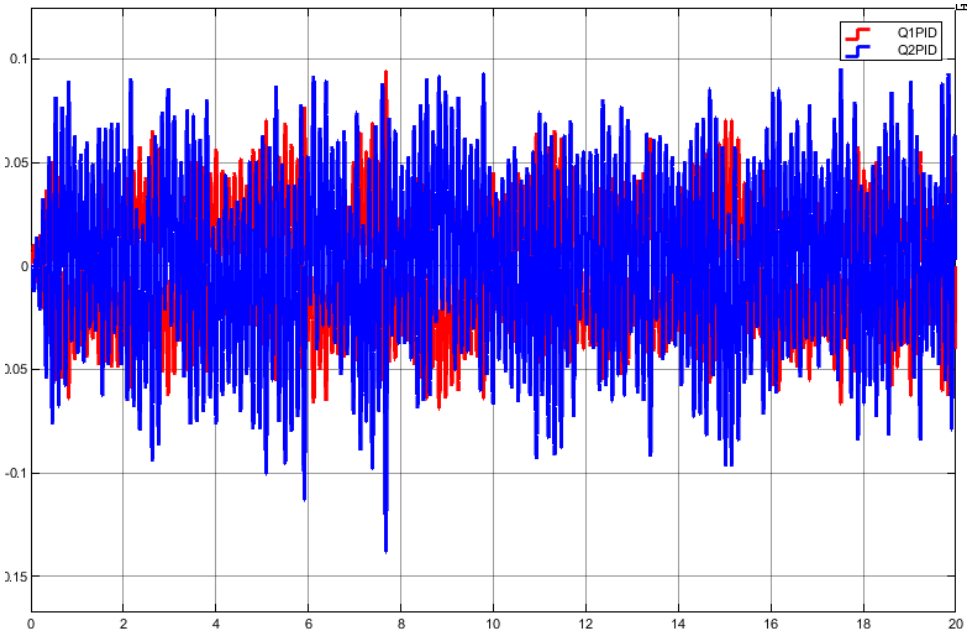

Figure 53 Experimental response of the PID controller

The LQG controller has a smoother response and does not require the LQG gain tuned. Applying the tuned gain with a value of 1.07 the system keeps oscillating about a value of -2 to 2 degrees. The response of the system can be observed in the following figure.

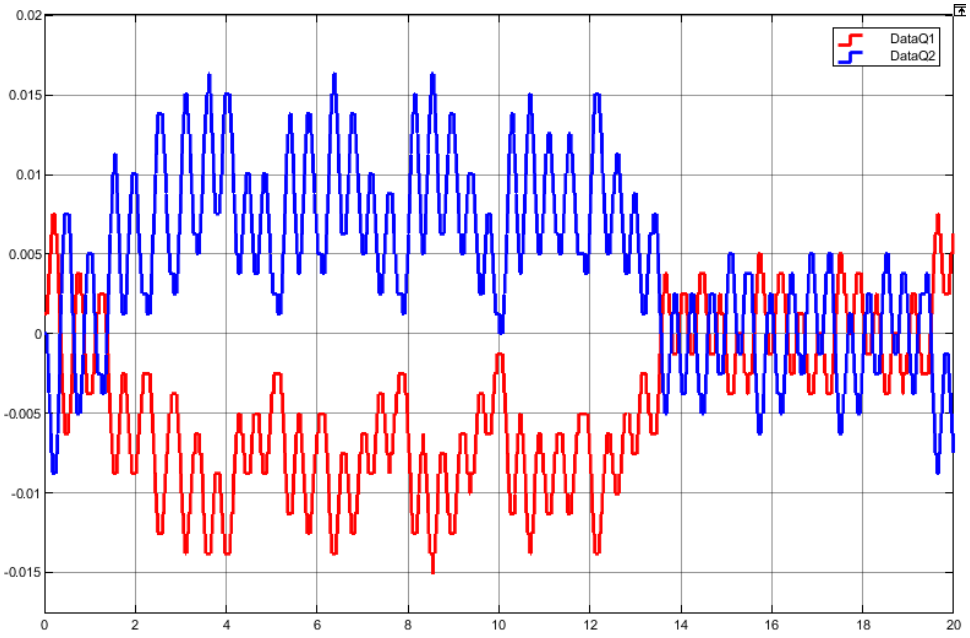

Figure 54Experimental response of the LQG controller

The Response of the H infinity is the smoother one of the controllers. With a tuned gain of a value of 0.95 that is the most optimal for delay tolerance. With this gain, the system oscillates between -1.2 to 1.2 degrees. The obtained data of this controller is the following one.

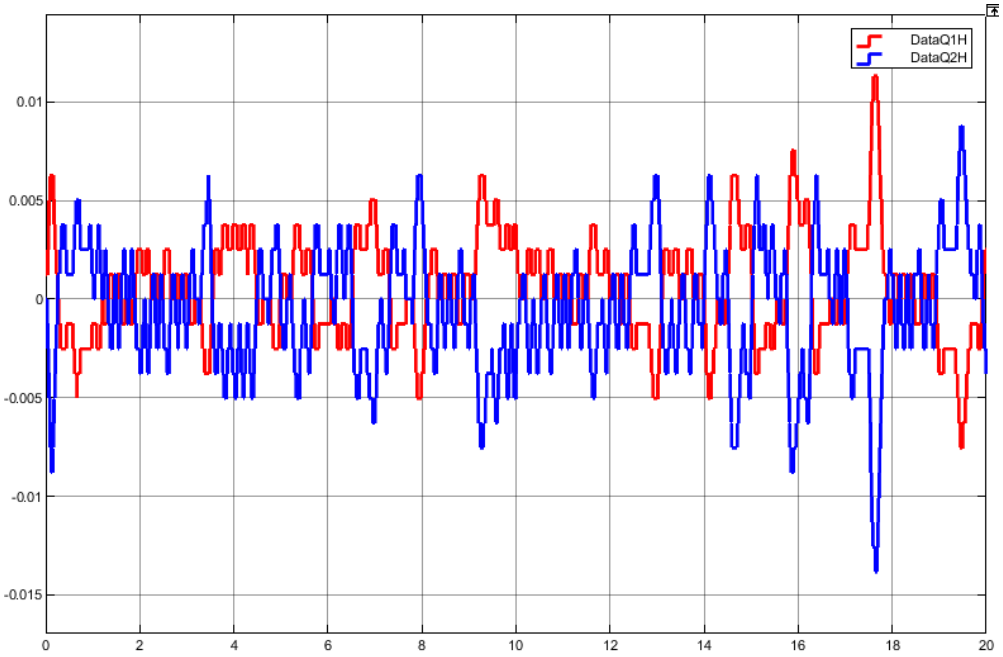

Figure 55 Experimental response of the H infinity controller

Applying the delay using the delay with a resolution of 1 [ms] the following table with results was obtained.

Table 10 Comparison of the delay response

Parameter	*Calculated value(linear)*	*Calculated value(non linear)*	*Experimental value*
$Maximum\ delay\ for\ PID$	3.5ms	3.54	3 ms
$Maximum\ delay\ for\ LQG$	17.56 ms	17.4	15 ms
$Maximum\ delay\ for$ H∞	12.51 ms	12.4	10 ms

The error presented on these values could be caused by the inner delay of the motor driver, the non-linearities ignored for the mathematical modeling, or the linearization process.

14. Conclusions

After the development of the process, it was observed some facts that have to be remarked. One of the first facts is although the mathematical modeling has accuracy the linearization of the process reduces the reaching of the controllers making that if the system pass from the range of -10 to 10 degrees the stability cannot be recovered.

Another interesting fact was that the LQG and the LQR model has significant differences between them this could be because the model is highly nonlinear and the dynamic of the observer is not fast enough in comparison to the controller dynamics

Analyzing the behavior of the controllers against the delay tolerance it was observed that the PID has the lower tolerance of the three controllers but has the higher improvement by the delay schedule, this could be caused by the simplicity of their structure.

By the literature research, it was observed that the stable systems can be improved with delay scheduling more than the unstable systems. This is because the stable system has more probability to have more stability pockets than the unstable

The order of the H infinity controller is the main disadvantage of this controller at the moment to apply the delay scheduling, this is because it increases the computational time of the delay scheduling calculation up to 20 hours in a desktop computer with the following specifications:

- 16 GB RAM DDR4 3200Mhz
- Ryzen 5 3400G 4.0 Ghz
- Graphic Card Radeon VEGA 11
- Windows 10

This project mainly evidence that the more complex controller cannot be improved significantly by the uses of the delay scheduling as was observed obtaining only a 5 % increasing of the tolerances delay in comparison to the PID that gets an improvement of a 1000% on the delay tolerance.

Also was observed that the CTCR method is very accurate between the nonlinear model and the linear model, but in the real system a difference of the 16 % is observed.

15. Results

The results that will be obtained in the project are the following:

- Proceeding paper of IMECE 2020 conference. Already submitted. Oral presentation scheduled by November 15-18, 2020. Portland, Oregon, USA. *"*Robust control of a Pendubot improved with delayed scheduling*".*
- Proceeding paper of CIIMA 2021 conference. Already submitted. Oral presentation scheduled by October 28, 2021. Bucaramanga, Santander, Colombia.

"DELAY SCHEDULING OF A LQR AND PID CONTROLLED PENDUBOT USING CTCR METHOD". by helio Schneider., Carlos Borrás., Nejat Olgac., ASME-IMECE2020-Portland,Oregon ., USA.

- Functional experimental prototype with datasheet. (design of the two link underactuated planar robot called Pendubot)
- New Matlab libraries for "Delay scheduling".
- Final Document (Master Thesis)with all the generated knowledge

16. Budget

Table 2. Budget of the project.

Concept	**Category**	**Cost (COP)**
Project´s Director	Human resource (64 weeks)	7.680.000
Principal Investigator	Human resource (64 weeks full time)	26.334.090
Laptop	Hardware	1.800.000
Arduino Due	Hardware(Procesador pendubot)	162.400
Encoder	Hardware(sensorica)	337.218
Matlab License	Software	3.522.057
Word License	Software	440.000
Papers bibliography	Literature cost	880.000
Total Cost		$41.155.765.oo

17. Bibliography

[1]. Olgac, N., & Sipahi, R. (2002). An Exact Method for the Stability Analysis of Time-Delayed Linear Time-Invariant (LTI) Systems. 47(5), 793–797.

[2]. Spong, M. W., & Block, D. J. (1995). Pendubot: a mechatronic system for control research and education. *Proceedings of the IEEE Conference on Decision and Control*, *1*(December), 555–556. https://doi.org/10.1109/cdc.1995.478951

[3]. Cavdaroglu, M. E., & Olgac, N. (2009). Full-state feedback control design with "delay scheduling" for cart-and-pendulum dynamics. *IFAC Proceedings Volumes (IFAC-PapersOnline)*, *8*(PART 1), 296–302. https://doi.org/10.1016/j.mechatronics.2010.08.007

[4]. Sipahi, R., & Olgac, N. (2005). Complete stability robustness of third-order LTI multiple time-delay systems. *Automatica*, *41*(8), 1413–1422. https://doi.org/10.1016/j.automatica.2005.03.022

[5]. Zhang, M., & Tarn, T. J. (2002). Hybrid control of the Pendubot. *IEEE/ASME Transactions on Mechatronics*, *7*(1), 79–86. https://doi.org/10.1109/3516.990890

[6]. Sergio, S., Soto, I., & Campa, R. (n.d.). *Modeling and Control of a Pendubot with Static Friction*. 229–240. https://doi.org/10.1007/978-3-319-09858-6

[7]. Olgac, N., Sipahi, R., & Ergenc, A. F. (2007). "Delay scheduling", an unconventional use of time delay for trajectory tracking. *Mechatronics*, *17*(4–5), 199–206. https://doi.org/10.1016/j.mechatronics.2007.02.001

[8]. Ogata, K., Pinto Bermúdez, E., Matía, F., Pearson, E., Hall, P., Dorf, R. C., & Pearson, R. H. B. (n.d.). *Ingeniería de control moderna www.elsolucionario.net*. Retrieved from www.pearsoneducacion.com

[9]. Olgac, N., Ergenc, A. F., & Sipahi, R. (2005). "Delay scheduling": A new concept for stabilization in multiple delay systems. *JVC/Journal of Vibration and Control*, *11*(9), 1159–1172. https://doi.org/10.1177/1077546305055777

[10]. Olgac, N., Vyhlídal, T., & Sipahi, R. (2006). Exact stability analysis of neutral systems with cross-talking delays. In *IFAC Proceedings Volumes (IFAC-PapersOnline)* (Vol. 6). https://doi.org/10.3182/20060710-3-IT-4901.00029

[11]. Albertos, P., & Garcia, P. (2007). Dead-time compensation in discrete time control. *Systems Science*, *33*(January 2007), 13–20.

[12]. Banerjee, R., & Pal, A. (2018). Stabilization of Inverted Pendulum on Cart Based on LQG Optimal Control. *2018 International Conference on Circuits and Systems in Digital Enterprise Technology, ICCSDET 2018*, 5–8. https://doi.org/10.1109/ICCSDET.2018.8821243

[13]. Brian, A., & Jhon, M. (1990). Optimal Control: Linear Quadratic Methods. In *Proceedings of the IEEE*.

[14]. Cavdaroglu, M. E., & Olgac, N. (2009). Full-state feedback control design with "delay scheduling" for cart-and-pendulum dynamics. In *IFAC Proceedings Volumes (IFAC-PapersOnline)* (Vol. 8, Issue PART 1). IFAC. https://doi.org/10.3182/20090901-3-ro-4009.00048

[15]. Davison, D. E., & Tonita, R. (2005). Performance limitations in control systems with sensor time delays. *IFAC World Congress*, *16*(1), 225–230. https://doi.org/10.3182/20050703-6-cz-1902.00608

[16]. Glover, K. (2020). H-infinity control. *Encyclopedia of Systems and Control*, 1–9. https://doi.org/10.1007/978-1-4471-5102-9

[17]. Lee, Y., Lee, J., & Park, S. (2000). PID controller tuning for integrating and unstable processes with time delay. *Chemical Engineering Science*, *55*(17), 3481–3493. https://doi.org/10.1016/S0009-2509(00)00005-1

[18]. Matausek, M. R., & Micic, A. D. (1999). On the modified Smith predictor for controlling a process with an integrator and long dead-time. *IEEE Transactions on Automatic Control*, *44*(8), 1603–1606. https://doi.org/10.1109/9.780433

[19]. MatLab. (n.d.). *Linear-Quadratic-Gaussian (LQG) design - MATLAB lqg - MathWorks América Latina*. Retrieved November 1, 2021, from https://la.mathworks.com/help/control/ref/ss.lqg.html

[20]. Mazenc, F., & Niculescu, S. I. (2001). Lyapunov stability analysis for nonlinear delay systems. *Systems and Control Letters*, *42*(4), 245–251. https://doi.org/10.1016/S0167-6911(00)00093-1

[21]. Montoro López, G. (1996). Contribución al estudio y desarrollo de técnicas de control aplicadas a la linealización de sistemas. In *TDX (Tesis Doctorals en Xarxa)*. http://hdl.handle.net/2117/94219

[22]. Murray, R., Li, Z., & Sastry, S. (1994). A mathematical introduction to robotic manipulation. In *Book* (Vol. 29). /citations?view_op=view_citation&continue=/scholar%3Fhl%3Den%26start%3D140%26as_sdt%3D0,5%26scilib%3D1&citilm=1&citation_for_view=OZNzz9gAAAAJ:35N4QoGY0k4C&hl=en&oi=p

[23]. Ogata, K. (2010). Modern control engineering.

[24]. Olgac, N., & Sipahi, R. (1995). An exact method for the stability analysis of time-delayed linear time-invariant (LTI) systems. *IEEE Transactions on Automatic Control*, *47*(5), 793–797. https://doi.org/10.1109/TAC.2002.1000275

[25]. Roh, Y.-H., & Oh, J.-H. (1999). Robust stabilization of uncertain input-delay systems by sliding mode control with delay compensation. *Automatica*, *35*(10), 1861–1865. https://doi.org/10.1016/S0005-1098(01)00124-8

[26]. Sipahi, R., & Olgac, N. (2005). Complete stability robustness of third-order LTI multiple time-delay systems. *Automatica*, *41*(8), 1413–1422. https://doi.org/10.1016/j.automatica.2005.03.022

[27]. Spong, M. W., & Block, D. J. (1995). Pendubot: a mechatronic system for control research and education. *Proceedings of the IEEE Conference on Decision and Control*, *1*(December), 555–556. https://doi.org/10.1109/cdc.1995.478951

[28]. *Web of Science*. (n.d.). Retrieved November 3, 2021, from https://access.clarivate.com/login?app=wos&alternative=true&shibShireURL=https:%2F%2Fwww.webofknowledge.com%2F%3Fauth%3DShibboleth&shibReturnURL=https:%2F%2Fwww.webofknowledge.com%2F&roaming=true

[29]. Zhang, M., & Tarn, T. J. (2002). Hybrid control of the Pendubot. *IEEE/ASME Transactions on Mechatronics*, *7*(1), 79–86. https://doi.org/10.1109/3516.990890

[30]. Žilić, T., Pavković, D., & Zorc, D. (2009). Modeling and control of a pneumatically actuated inverted pendulum. *ISA Transactions*, *48*(3), 327–335. https://doi.org/10.1016/j.isatra.2009.03.004